Novel intracellular phospholipase B from *Pseudomonas aeruginosa* with activity towards endogenous phospholipids affects biofilm assembly

Andrea J. Weiler[1], Olivia Spitz[2], Mirja Gudzuhn[3], Stephan N. Schott-Verdugo[4,5], Michael Kamel[6], Björn Thiele[8], Wolfgang R. Streit[3], Alexej Kedrov[6], Lutz Schmitt[2], Holger Gohlke[4,7] and Filip Kovacic[1,*]

1. Institute of Molecular Enzyme Technology, Heinrich Heine University Düsseldorf, Forschungszentrum Jülich GmbH, D-52425 Jülich, Germany
2. Institute of Biochemistry, Heinrich-Heine-University Düsseldorf, 40225 Düsseldorf, Germany
3. Department of Microbiology and Biotechnology, University of Hamburg, Ohnhorststr. 18, 22609 Hamburg, Germany
4. Institute for Pharmaceutical and Medicinal Chemistry, Heinrich Heine University Düsseldorf, 40225 Düsseldorf, Germany
5. Centro de Bioinformática y Simulación Molecular (CBSM), Facultad de Ingeniería, Universidad de Talca, 2 Norte 685, CL-3460000 Talca, Chile
6. Synthetic Membrane Systems, Institute of Biochemistry, Heinrich Heine University Düsseldorf, 40225 Düsseldorf, Germany
7. John von Neumann Institute for Computing (NIC), Jülich Supercomputing Centre (JSC) & Institute of Biological Information Processing (IBI-7: Structural Biochemistry), Forschungszentrum Jülich GmbH, 52425 Jülich, Germany
8. Institute of Bio- and Geosciences, Plant Sciences (IBG-2) and Agrosphere (IBG-3), Forschungszentrum Jülich GmbH, D-52425 Jülich, Germany

* Corresponding author: f.kovacic@fz-juelich.de

Keywords: oligomerization, virulence factor, membrane protein, α/β-hydrolase, pathogen

Abstract

Pseudomonas aeruginosa is a severe threat to immunocompromised patients due to its numerous virulence factors and multiresistance against antibiotics. This bacterium produces and secretes various toxins with hydrolytic activities including phospholipases A, C and D. However, the function of intracellular phospholipases for bacterial virulence has still not been established. Here we demonstrate that the hypothetical gene *pa2927* of *P. aeruginosa* encodes a novel phospholipase B named PaPlaB. PaPlaB isolated from detergent-solubilized membranes of *E. coli* rapidly degraded various GPLs including endogenous GPLs isolated from *P. aeruginosa* cells. Cellular localization studies suggest that PaPlaB is peripherally bound to the inner and outer membrane of *E. coli*, yet the active form was predominantly associated with the cytoplasmic membrane. *In vitro* activity of purified and detergent-stabilized PaPlaB increases at lower protein concentrations. The size distribution profile of PaPlaB oligomers revealed that decreasing protein concentration triggers oligomer dissociation. These results indicate that homooligomerisation regulates PaPlaB activity by a yet unknown mechanism, which might be required for preventing bacteria from self-disrupting the membrane. We demonstrated that PaPlaB is an important determinant of the biofilm lifestyle of *P. aeruginosa*, as shown by biofilm quantification assay and confocal laser scanning microscopic analysis of biofilm architecture. This novel intracellular phospholipase B with a putative virulence role contributes to our understanding of membrane GPL degrading enzymes and may provide a target for new therapeutics against *P. aeruginosa* biofilms.

1. Introduction

Pseudomonas aeruginosa causes severe hospital-associated infections, especially in immunocompromised hosts, which are complicated to treat due to the increasing antibiotic resistance and the aggressive nature of this pathogen leading to the fast progression of the infection [1, 2]. In general, the overall mortality rate determined on a large group of 213,553 patients with *P. aeruginosa* septicemia was 16 %, going along with the observation that the incidence of sepsis increases since 2001 [3]. This clearly illustrates a need for novel treatments to kill the pathogen or, at least, diminish its virulence. Therefore, WHO has recently classified *P. aeruginosa* in the group of most critical pathogens [1] and advised research and development of new antibiotics against it. Unfortunately, despite intensive investigations towards understanding virulence in this human pathogen, many genes encoding putative virulence factors remain uncharacterized [4].

In *P. aeruginosa*, as well as in other bacterial pathogens, phospholipases, the hydrolases with membrane phospholipid-degrading activity, play an important role during infections. They are classified into several groups depending on which ester bond of a glycerophospholipid (GPL) they hydrolyze [5]. While phospholipases C (PLC) and D (PLD), respectively, hydrolyze the glycerol-oriented and the head group-oriented phosphodiester bonds of phospholipids, phospholipases A1 (PLA1) and A2 (PLA2) release fatty acids bound at the *sn*-1 or *sn*-2 positions, respectively. Phospholipases B (PLB) cleave *sn*-1 and *sn*-2 bonds of GPL with similar specificity. Lysophospholipids, degradation products of PLA1 and PLA2, are converted by lysophospholipases A (lysoPLA) to glycerophosphoalcohol and fatty acid.

The contribution of bacterial phospholipases to virulence is predominantly related to damaging the host cells, which mostly enhances the survival and spread of the pathogen in the host [6, 7]. Several phospholipases of *P. aeruginosa*, namely phospholipases A ExoU [8] and PlaF [9, 10],

phospholipase A/esterase EstA [11], phospholipase C PlcH [12], and two phospholipases D, PldA and PldB [13], were suggested to be virulence factors in that way. The ExoU, PldA, and PldB are directly secreted into eukaryotic cells, where they modulate native host pathways to facilitate invasion by *P. aeruginosa* or inflammation [14]. An EstA of *P. aeruginosa,* which is anchored to the outer membrane with the catalytic domain protruding into the extracellular medium, was shown to effects virulence- and resistance-related phenotypes (cell motility and biofilm formation) [11]. PlcH, one of three secreted PLCs of *P. aeruginosa*, is considered as a virulence factor because (i) it exhibits hemolytic activity; (ii) it is produced during clinical infection with *P. aeruginosa* [15], and (iii) *plcH* deletion strain of *P. aeruginosa* shows attenuated virulence in mouse burn models [16]. However, despite more than three decades of research on phospholipases, still little is known about the direct action of *P. aeruginosa* phospholipases on their membranes.

On the contrary, one of the best-studied pathogens concerning phospholipases is *Legionella pneumophila,* an intracellularly replicating Gram-negative bacterium [17]. Several phospholipases of *L. pneumophila* were proposed to have a function for establishing a proper life cycle inside a host. One of them is the major surface-associated phospholipase PlaB (LpPlaB). LpPlaB is a serine hydrolase with hemolytic activity and catalytic activity towards common bacterial phospholipids and lysophospholipids containing glycerol and choline head groups [18, 19]. However, the catalytic mechanism of LpPlaB, the mechanism of targeting to the outer membrane, structural features responsible for binding to the membrane, and its effect on the host are unknown.

Here, we expressed, purified, and characterized a homolog of LpPlaB from human pathogen *P. aeruginosa* PA01, which we named PaPlaB. Comprehensive phospholipolytic enzyme activity studies revealed that PaPlaB is a promiscuous PLB and lysoPLA, which shows strong activity towards endogenous phospholipids isolated from *P. aeruginosa*. Furthermore, we demonstrated that a *P. aeruginosa* Δ*plaB* deletion strain produces less biofilm with a different architecture

compared to the wild-type bacterium. Thus, the PaPlaB is a novel putative virulence factor of *P. aeruginosa* PA01 belonging to the poorly understood PLB family.

2. Material and methods

2.1. Sequence analysis, and structure prediction

Amino acid sequence search and alignment were performed using BLAST and alignment tools provided by the National Center for Biotechnology Information (www.ncbi.nlm.nih.gov) [20]. The sequence alignment was visualized using BioEdit software [21]. The secondary structure was predicted with the JPred4 server using a method based on hidden Markov models [22]. TMpred server (https://embnet.vital-it.ch/software/TMPRED_form.html) was used to predict transmembrane helices with the length between 17 and 33 residues. The homology-based structural model of PaPlaB was built using the Phyre2 server [23], and the TopScore tool [24] was used to validate the structure prediction.

For further validation, protein residue-residue contacts were calculated with MetaPSICOV2 server [25] using a large sequence alignment containing 3,469 sequences. A distance violation (DV) score which indicates deviation (higher score higher deviation) between the MetaPSICOV2 predicted contacts and those found in the Phyre2 model was computed according to eq. 1. Hence, DV score below 10 indicates that a structural model has the same fold as the native structure [26].

$$DV = \frac{1}{L}\sum_{i=1}^{L}\sum_{j>i}^{L} score_{ij} \qquad score_{ij} = \begin{cases} d_{ij} - 8, if\ d_{ij} > 8\ \text{Å} \wedge P > 0.5 \\ 0, if\ \left(d_{ij} \leq 8\ \text{Å} \wedge\ P > 0.5\right) \vee P < 0.5 \end{cases} \quad \text{(eq. 1)},$$

where L is the sequence length, d_{ij} is the distance between C_β atoms of the corresponding residue pair (C_α if glycine is used), and P is the MetaPSICOV2 prediction confidence bounded between 0 and 1. The structures of oligomers were generated by *ab initio* docking of the monomeric structure followed by structural refinement using the GalaxyHOMOMER server [27].

Refined structures of PaPlaB homooligomers were used for positioning them in the membrane with PPM web server provided by Orientations of Proteins in Membranes (OPM) database [28]. The PyMol software (The PyMOL Molecular Graphics System, Version 1.2r3pre, Schrödinger, LLC.) was used for visualization of the structural model.

2.2. Molecular cloning

The *paplaB* gene containing the sequence that encodes a C-terminal His_6-tag was amplified using Phusion® DNA polymerase (Thermo Fisher Scientific, Darmstadt, Germany). In the PCR, the genomic DNA of *P. aeruginosa* PA01 [29], isolated with the DNeasy blood and tissue kit (QIAGEN, Germany), was used as the template together with primers paplaB_for and paplaB_rev (Table S1). The pET22-*paplaB* vector for T7 RNA polymerase-controlled expression of *paplaB* was constructed by ligation of the *paplaB* gene into the pET22b vector (Novagen, Germany) at *Nde*I and *Sac*I restriction sites, using T4 DNA ligase (Thermo Fisher Scientific). Site-directed mutagenesis of PaPlaB was performed by the Quick® Change PCR method using the pET22-*paplaB* plasmid as a template and complementary mutagenic oligonucleotide pairs (Table S1) [30]. *E. coli* DH5α strain [31] was used for molecular cloning experiments. The plasmid DNA and DNA fragments from the agarose gel (1 % w/v) after electrophoresis were isolated with innuPREP Plasmid Mini Kit 2.0 and the innuPREP DOUBLEpure Kit (Analytik Jena, Germany). Oligonucleotides synthesis and plasmid DNA sequencing was performed by Eurofins Genomics (Germany).

2.3. Protein expression and purification

For the expression of PaPlaB with a C-terminal His_6-tag, *E. coli* C43(DE3) [32] cells were transformed with pET22-*paplaB* plasmid, and the empty pET22b vector was used as a control. Cells were grown overnight in lysogeny broth (LB) medium [33] supplemented with ampicillin (100 µg/ml) at 37°C with agitation. Overnight cultures were used to inoculate the expression cultures to an initial OD_{580nm} = 0.05 in LB medium containing ampicillin (100 µg/ml). The cultures

were grown at 37°C, and the expression of *paplaB* was induced with isopropyl-β-D-thiogalactoside (IPTG, 1 mM) at OD_{580nm} = 0.4 - 0.6 followed by incubation at 37°C for 5 hours. The cells were harvested by centrifugation (6,000 *g*, 4°C, 10 min) and stored at -20° C before proceeding with further analysis. Active site variants of PaPlaB carrying S79A, D196A, or H244A mutations were expressed the same as the PaPlaB.

Cells producing PaPlaB were suspended in 100 mM Tris-HCl pH 8, disrupted by a French press, and incubated for 30 min with lysozyme (2 mg/ml) and DNase (0.5 mg/ml). The cell debris and inclusion bodies were removed by centrifugation (6,000 *g*, 4°C, 10 min), and the soluble cell lysate was ultracentrifuged (180,000 *g*, 4°C, 2 h) to isolate the membrane fraction. Subsequently, the proteins were extracted from the membranes upon overnight incubation in the solubilization buffer (5 mM Tris-HCl pH 8, 300 mM NaCl; 50 mM KH_2PO_4; 20 mM imidazole, Triton X-100 1 % v/v) at 4°C. Insoluble debris was removed by ultracentrifugation (180,000 *g*, 4°C, 0.5 h), and the supernatant containing PaPlaB was used for purification.

Immobilized metal affinity chromatographic purification of PaPlaB was performed [34] using the ÄKTA Pure instrument (GE Healthcare). The Ni^{2+}-NTA column (4 ml; Macherey-Nagel, Düren) was equilibrated with ten column volumes of the solubilization buffer before loading the sample. The column was washed with five column volumes of the washing buffer (5 mM Tris-HCl pH 8, 300 mM NaCl, 50 mM KH_2PO_4, 50 mM imidazole, 0.22 mM DDM) to remove unspecifically bound proteins followed by the elution of PaPlaB with 100 ml of buffer (5 mM Tris-HCl pH 8, 300 mM NaCl, 50 mM KH_2PO_4, 0.22 mM DDM) in which the concentration of imidazole was increased linearly from 50 to 500 mM. The fractions containing pure PaPlaB were transferred into 100 mM Tris-HCl, pH 8 supplemented with 0.22 mM DDM by gel filtration using the PD-10 column (GE Healthcare). Samples were concentrated using Amicon®Ultra-4 ultrafiltration device, cut-off 10 kDa (Merck

Millipore). The protein was incubated at 4°C for 1 h with Bio-Beads™ SM-2 resin (Bio-Rad) equilibrated with 100 mM Tris-HCl, pH 8 to remove excess of detergent.

2.4. *In vitro* separation of inner and outer membranes

The separation of the inner and outer membranes of *E. coli* C43(DE3) pET22-*paplaB* (25 ml LB medium, 37°C, 5 h after induction) was performed with a continuous sucrose gradient (20 - 70 % w/v in 100 mM Tris-HCl pH 7.4). The gradients were prepared in SW40-type tubes (Beckman Coulter) using the Gradient Station (Biocomp Instruments, Canada). Isolated membranes were suspended in buffer containing 20 % (w/v) sucrose and loaded on the top of the continuous sucrose gradient followed by ultracentrifugation at 110,000 *g* for 16 h, 4°C in swinging-bucket rotor SW40 (Beckman Coulter). Fractions (1 ml) were collected from the top using the Gradient Station equipped with a TRIAX UV-Vis flow-cell spectrophotometer (Biocomp Instruments, Canada). The sucrose concentration in collected fractions was determined with a refractometer (OPTEC, Optimal Technology, Baldock UK).

2.5. SDS-PAGE and immunodetection

The sodium dodecyl sulfate-polyacrylamide gel electrophoresis (SDS-PAGE) was performed according to the method of Laemmli [35], and the gels were stained with Coomassie Brilliant Blue G-250. For immunodetection of PaPlaB, the gel was loaded with 10 µl of the cell, soluble and membrane fractions isolated from the cell suspension with OD_{580nm} = 25. After SDS-PAGE, proteins were transferred from the gel onto a polyvinylidene difluoride membrane [36] and detected with the anti-His (C-terminal)-HRP antibody (Thermo Fisher/Invitrogen) according to the manufacturer's instructions. The concentration of PaPlaB was determined using the UV-VIS spectrophotometer NanoDrop 2000c (Thermo Fisher Scientific). The extinction coefficient ε = 73.005 M^{-1} cm^{-1} was calculated with the ProtParam tool [37].

2.6. Enzyme activity assay and inhibition

Esterase activity of PaPlaB was determined in a 96-well microtiter plate (MTP) at 37°C by combining 10 µl of enzyme sample with 150 µl of the *p*-nitrophenyl butyrate (*p*-NPB) substrate [5]. Hydrolytic activities towards glycerophospholipids (GPLs) and lysoGPLs (Table S2), which were purchased from Avanti Polar lipids (Alabaster, USA), were determined by quantification of released fatty acids using NEFA assay kit (Wako Chemicals, Neuss, Germany) [5]. Lipids were dissolved in NEFA buffer (50 mM Tris, 100 mM NaCl, 1 mM $CaCl_2$, 1 % (v/v) Triton X-100, pH 7.2). The enzymatic reactions were performed by combining 12.5 µl of enzyme sample with 12.5 µl of a lipid substrate (0.67 mM) at 37°C for 15 min. The fatty acid amount was calculated from the calibration curve made with 0.5, 1, 2, 3, 4, and 5 nmol oleic acid.

The inhibition of PaPlaB with PMSF, paraoxon (both were dissolved in propane-2-ol), and EDTA (dissolved in 100 mM Tris-HCl pH 8) was tested as described previously [9]. Inhibition of PaPlaB was performed by incubating enzyme aliquots with the inhibitors for 1.5 h at 30°C, followed by determination of the enzymatic activity using the *p*-NPB substrate.

Phospholipase A1 (PLA1) and phospholipase A2 (PLA2) activities of PaPlaB were measured using selective fluorescent substrates PED-A1, [N-((6-(2,4-DNP)amino)hexanoyl)-1-(BODIPY®FL C5)-2-hexyl-*sn*-glycero-3-phosphoethanolamine]; PC-$A2_{R/G}$, 1-O-(6-BODIPY®558/568-aminohexyl)-2-BODIPY®FL C5-*sn*-glycero-3-phosphocholine (Thermo Fisher Scientific) as described previously [38]. Measurements in 96-well MTP were performed at 25°C by combining 50 µl of the substrate with 50 µl PaPlaB, or control enzymes, the PLA1 of *Thermomyces lanuginosus* (5 *U*/ml) and the PLA2 or *Naja mocambique mocambique* (0.7 *U*/ml).

2.7. Gas chromatography-mass spectrometric (GC-MS) analysis of fatty acids

Fatty acids were extracted after incubation of purified PaPlaB (2 ml, 4.28 µg/ml) with 1-oleoyl-2-palmitoyl-PC ($PC_{18:1\text{-}16:0}$) (0.5 mM in 2 ml NEFA buffer) for 1 h at 37°C. After incubation 1 ml of

NEFA buffer was added, and fatty acids were extracted with 12 ml $CHCl_3$: CH_3OH = 2 : 1. The $CHCl_3$ extract was removed, and FAs were extracted again with 8 ml $CHCl_3$. $CHCl_3$ extracts were combined and evaporated.

FAs were dissolved in 200 µl $CHCl_3$. The $CHCl_3$ extract was mixed with ten volumes of acetonitrile and filtered through a 0.2 µm pore size filter. The residues of the PaPlaB extracts were dissolved in 1 ml acetonitrile : methylenchloride = 4 : 1. Before GC-MS analysis, fatty acids in the PaPlaB extracts and standard solutions were derivatized to their trimethylsilylesters. For this purpose, 100 µl of each sample solution was mixed with 700 µl acetonitrile, 100 µl pyridine and 100 µl N-methyl-N-(trimethylsilyl) trifluoroacetamide and heated to 90°C for 1 h. A 1 mM fatty acid mixture in acetonitrile ($C_{10:0}$-, $C_{12:0}$-, $C_{14:0}$-, $C_{16:0}$-, $C_{18:0}$- and $C_{18:1}$-fatty acid (oleic acid)) was diluted to 50, 100, 200 and 400 µM and derivatized in the same manner as above. The GC-MS system consisted of an Agilent gas chromatograph 7890A and autosampler G4513A (Agilent, CA, USA) coupled to a TOF mass spectrometer JMS-T100GCV AccuTOF GCv (Jeol, Tokyo, Japan). Analytes were separated on a Zebron-5-HT Inferno column (30 m x 0.25 mm i.d., 0.25 µm film thickness, Phenomenex, USA). Helium was used as carrier gas at a constant gas flow of 1.0 ml/min. The oven temperature program employed for analysis of silylated fatty acids was as follows: 80°C; 5°C/min to 300°C, held for 1 min. The injector temperature was held at 300°C, and all injections (1 µl) were made in the split mode (1:10). The mass spectrometer was used in the electron impact (EI) mode at an ionizing voltage of 70 V and ionizing current of 300 µA. Analytes were scanned over the range m/z 50 - 750 with a spectrum recording interval of 0.4 s. The GC interface and ion chamber temperature were both kept at 250°C. After the conversion of the raw data files to the cdf-file format, data processing was performed by the use of the software XCalibur 2.0.7 (ThermoFisher Scientific). Fatty acids from the PaPlaB sample were identified by comparison of their retention times and mass spectra with those of fatty acid standards.

2.8. Thermal stability analysis

Differential scanning fluorimetric analysis of PaPlaB thermal stability was performed using the Prometheus NT.48 nanoDSF instrument (NanoTemper Technologies, Germany) [39]. The Prometheus NT.Plex nanoDSF Grade Standard Capillary Chip containing 10 µl PaPlaB sample per capillary was heated from 20°C to 90°C at the rate of 0.1°C/min, and the intrinsic fluorescence at wavelengths of 330 nm and 350 nm was measured. The first derivative of the ratio of fluorescence intensities at 350 nm and 330 nm as a function of temperature was used to visualize the denaturing transition and determine the "melting" temperature. Enzyme activity-based thermal stability experiments were performed by measuring the residual esterase activity of a PaPlaB sample incubated 1 h at temperatures from 30°C to 70°C [40]. After the incubation, the enzymatic assay was performed as described above using the *p*-NPB substrate, and the inactivation temperature was determined.

2.9. Multi-angle light scattering (MALS) and size-exclusion chromatography

Superdex 200 Increase 10/300 GL column (GE Healthcare) was equilibrated overnight at a flow rate of 0.6 ml/min with 100 mM Tris pH 8 containing 0.22 mM DDM. For each analysis 200 µl PaPlaB at concentrations of 1, 0.5 and 0.1 mg/ml were loaded to the column at the flow rate of 0.6 ml/min using 1260 binary pump (Agilent Technologies), and the scattered light (miniDAWN TREOS II light scatterer, Wyatt Technologies) and the refractive index (Optilab T-rEX refractometer, Wyatt Technologies) were measured. Data analysis was performed with the software ASTRA 7.1.2.5 (Wyatt Technologies) under the assumption that dn/dc of DDM is 0.1435 ml/g and the extinction coefficient of PaPlaB is 1.450 ml/(mg*cm) [41].

Size-exclusion chromatographic (SEC) analysis of PaPlaB in Tris-HCl (100 mM, pH 8, 0.22 mM DDM) buffer was performed using Biosep-SEC-S3000 column (Phenomenex, Aschaffenburg, Germany), LC-10Ai isocratic pump (Shimadzu, Duisburg, Germany) and SPD-M20A photodiode array detector

(Shimadzu, Duisburg, Germany). The molecular weight (M_w) of standard proteins dissolved in the same buffer as PaPlaB was determined (Table S3). For the analysis, 100 µl of PaPlaB or protein standard sample was loaded on the column, and separation was achieved at a flow rate of 0.5 ml/min and 26°C.

2.10. Construction of *P. aeruginosa* Δ*plaB* strain

The *P. aeruginosa* Δ*plaB* mutant strain was generated by homologous recombination [42]. In short, *P. aeruginosa* PAO1 cells were conjugated with the pEMG-*ΔplaB* mutagenesis vector containing the 814 bp fragment of the upstream region of *paplaB*, followed by a gentamicin resistance gene and the 584 bp downstream region of *paplaB*. For that, *E. coli* S17-1 pir transformed with the pEMG-*ΔplaB* plasmid was used as a donor strain. *Pseudomonas* cells with pEMG-*ΔplaB* plasmid integrated on the chromosome were selected on LB-agar plates containing gentamicin (30 µg/ml), kanamycin (300 µg/ml; a kanamycin resistance gene is encoded on pEMG plasmid) and Irgasan (25 µg/ml; used for negative selection of *E. coli*). Cells transformed with the plasmid pSW-2 containing the I-*Sce*I restriction endonuclease were cultivated on LB agar plates containing benzoic acid (2mM; for induction of I-SceI expression) and Irgasan (25 µg/ml). The deletion of the *paplaB* gene was confirmed by PCR amplification using the genomic DNA of *P. aeruginosa ΔplaB* as the template (Fig. S1).

2.11. Fluorescence imaging of biofilm in flow chambers

P. aeruginosa PAO1 and Δ*plaB* biofilms were grown on a microscope cover glass (24 mm x 50 mm, thickness 0.17 mm, Carl Roth GmbH & Co. KG, Karlsruhe, Germany), which was fixed with PRESIDENT The Original light body silicon (Coltène/Whaledent AG, Altstätten, Switzerland) on the upper side of the three-channel flow chambers [43]. The flow chambers and tubes (standard tubing, ID 0.8 mm, 1/16" and Tygon Standard R-3607, ID 1.02 mm; Cole-Parmer GmbH, Wertheim, Germany) were sterilized by flushing with sterile chlorine dioxide spray (Crystel TITANIUM, Tristel

Solutions Ltd., Snailwell, Cambridgeshire, United Kingdom). Afterward, the flow chambers were filled with 1 % (v/v) sodium hypochlorite, and the tubes were autoclaved. All biofilm experiments were performed at 37°C with a ten-fold diluted LB medium. Before inoculation, the flow chamber was flushed with 1:10 diluted LB medium for 30 minutes with a flow rate of 100 µl/min using the IPC12 High Precision Multichannel Dispenser (Cole-Parmer GmbH, Wertheim, Germany). For inoculation, an overnight culture of *P. aeruginosa* PAO1 or Δ*plaB* was adjusted to an OD_{580nm} of 0.5 in 1:10 diluted LB medium. The diluted culture (300 µl) was inoculated in each channel. After the interruption of medium supply for 1 h, the flow (50 µl/min) was resumed, and the biofilm structure was analyzed after 24, 72, and 144 h grown at 37°C. For visualization, the cells were stained with propidium iodide and SYTO 9 dyes using the LIVE/DEAD™ BacLight™ Bacterial Viability Kit (Thermo Fisher Scientific). Imaging of biofilm was performed using the confocal laser scanning microscope (CLSM) Axio Observer.Z1/7 LSM 800 with airyscan (Carl Zeiss Microscopy GmbH, Germany) with the objective C-Apochromat 63x/1.20W Korr UV VisIR. The microscope settings for the different fluorescent dyes are shown in Table S4. The analysis of the CLSM images and three-dimensional reconstructions were done with the ZEN software (version 2.3, Carl Zeiss Microscopy GmbH, Germany). Experiments were repeated two times, each with one biological replicate that was analyzed at three different points by imaging a section of 100 x 100 µm.

2.12. Crystal violet biofilm assay

P. aeruginosa wild-type and Δ*plaB* cultures incubated in LB medium overnight at 37°C in Erlenmeyer flasks (agitation at 150 rpm) were used to inoculate 100 µl culture with OD_{580nm} 0.1 in plastic 96-well MTP. Cultures were grown at 37°C without agitation, and the cells attached to the surface of MTP after removing the planktonic cells were stained with 0.1 % (w/v) crystal violet solution for 15 min, solubilized with acetic acid (30 % v/v) and quantified spectrophotometrically [44].

3. Results

3.1 *P. aeruginosa* gene *pa2947* encodes a putative phospholipase A

We performed a BLAST search using sequences of the currently known bacterial PLAs to identify novel phospholipases A (PLA) in *P. aeruginosa* PA01 [6]. One of the results was a gene *pa2927* encoding a 49.5 kDa protein with moderate sequence similarity (39 %) to LpPlaB, a major intracellular PLA of *L. pneumophila* [18, 19, 45-48]. We named the *P. aeruginosa* homolog analogously, PaPlaB. A BLAST search revealed substantial sequence identity (27 to 43 %) between PaPlaB and several uncharacterized proteins and putative phospholipases (Figs. 1a and S2). The recently annotated active site of LpPlaB (Ser85, Asp203, His251) [18] allowed us to identify Ser79, Asp196, and His244 as residues of the putative catalytic triad in PaPlaB, which are strongly conserved among PaPlaB homologs (Fig. 1a). PaPlaB, similar to LpPlaB, contains the catalytic Ser79 embedded into a VHSTG pentapeptide, which differs from the canonical GXSXG lipase motif by the absence of the glycine at position -2 of the serine. The present threonine residue was shown to be functionally important, as the mutation T83G reduced LpPlaB activity by 95 % [18]. The difference in the catalytic pentapeptide was proposed to be a novel feature of the lipolytic family represented by LpPlaB [18]. Although no conserved domains encompassing the catalytic residues were identified in PaPlaB using either NCBI's conserved domain [49] or Pfam [50] databases, we observed a notably higher sequence identity of the 270 amino-terminal residues of PaPlaB to its homologs than the carboxy-terminal residues (271 – 443). Even secondary structure elements predicted in the N-terminal regions of PaPlaB and LpPlaB agreed better than secondary structure elements predicted in the C-terminal regions (Fig. S3).

To assess whether PaPlaB is a two-domain protein, we predicted its 3D structure with the Phyre2 homology modeling server [51]. Using the structure of a protein of unknown function from *Listera innocua* (PDB code: 3DS8) as a template, the homology model of the N-terminal PaPlaB domain

revealed an α/β-hydrolase fold, which provides a scaffold for the canonical serine-hydrolase catalytic triad (Fig. 1b) as found in many lipolytic enzymes [52, 53]. No homolog with a resolved structure was found for the C-terminal domain of PaPlaB. Therefore, the *ab initio* approach of the Phyre2 server was used. The resulting model for this domain suggested a four-stranded β-sheet (Fig. 1b) which was furthermore validated. Validation with TopScore [24] confirmed a higher quality of the N-terminal domain than the C-terminal one (Fig. 1c). Additional validation with a MetaPSICOV2 server shows two distinct groups of residue-residue contacts, one in the N-terminal and one in the C-terminal region, thus corroborating a two-domain protein structure (Fig. S4). DV score, a measure of the deviation of predicted contacts versus those derived from the structural model, of 2.7 suggests that the PaPlaB model has a fold similar to the native structure, as DV < 10 was calculated for real structures. In summary, our sequence, secondary and tertiary structure analyses indicate that PaPlaB has an N-terminal putative phospholipase A domain with an α/β-fold and a C-terminal domain, the function of which is currently unknown.

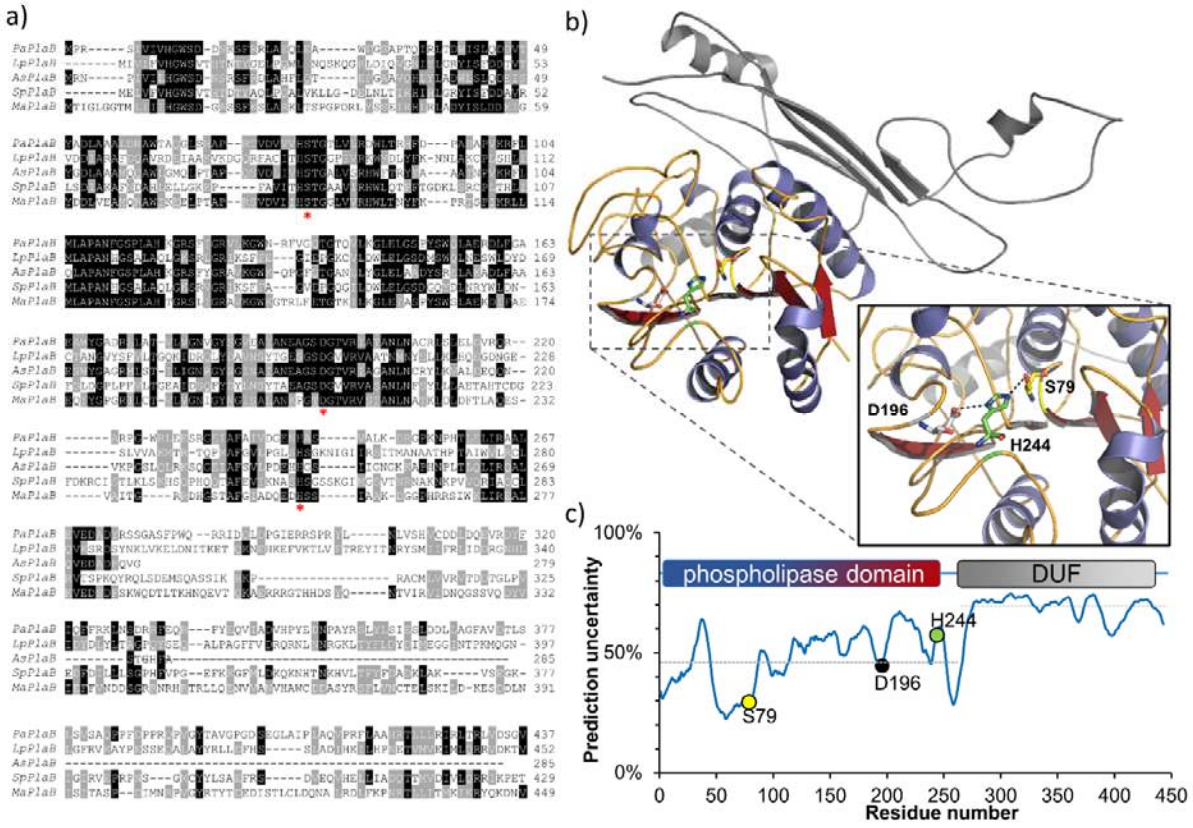

Fig. 1: Putative two-domain architecture of *P. aeruginosa* PaPlaB. a) Sequence alignment of PaPlaB from *P. aeruginosa* (PaPlaB), *Legionella pneumophila* (LpPlaB), *Alishewanella sp.32-51-5* (AsPlaB), *Shewanella pealeana* (SpPlaB), and *Marinobacter algicola* (MaPlaB). Black and grey background indicate identical and similar residues in at least three proteins, respectively. The catalytic triad residues (Ser79, Asp196, and His244 in PaPlaB) are marked with asterisks. The last six PaPlaB residues are shown in the Fig. S2. **b)** PaPlaB structural model. The N-terminal domain model (coloured secondary structure elements) was based on the structure of the protein of unknown function from *L. innocua* (PDB code: 3DS8). The C-terminal domain (grey) was modelled *ab initio* using the Phyre2 web server [51]. The view of the catalytic triad is expanded. **c)** The residue-wise uncertainty of the predicted PaPlaB model was computed with TopScore, a quality assessment tool for protein structure models [24]. Grey lines indicate average uncertainties of the phospholipase and DUF domains.

3.2 Expression of *paplaB* in *E. coli* yields a membrane-bound phospholipase A

To experimentally test the putative PLA function, we set out to heterologously express and purify PaPlaB. To achieve this, we constructed the PaPlaB expression vector (pET22-*paplaB*) suitable for heterologous expression in *E. coli* strains that contain the T7 RNA polymerase gene. *PaplaB* gene in pET22-*paplaB* plasmid was modified by including a sequence coding for six histidine residues at the 3' end to enable purification of the protein using immobilized metal affinity chromatography (IMAC) and the protein expression was conducted in *E. coli* C43(DE3) cells. SDS-PAGE (Fig. S5) and Western blot (Fig. 2) analyses of cells sampled during the first 5 h after induction revealed the expression of a protein with an estimated molecular weight (M_w) of ~50 kDa, which agrees with the theoretical M_w of PaPlaB (49.5 kDa). The expression of PaPlaB variants with mutated putative catalytic triad residues S79, D196, and H244 yielded also ~50 kDa proteins as shown by SDS-PAGE (Fig. S6a) and Western blot (Fig. S6b) analyses. Esterase activities of cell lysates revealed that the wild type PaPlaB was active while all three variants showed activities comparable to the activity of the empty vector control (Fig S6c)

Considering the membrane localization of the PaPlaB homolog from *L. pneumophila*, [19], we suspected a membrane localization of PaPlaB. This was confirmed by Western blot detection of PaPlaB only in the membrane fraction of *E. coli* C43(DE3) pET22-*paplaB* sedimented upon ultracentrifugation, while no PaPlaB was detected in the soluble fraction containing periplasmic and cytoplasmic proteins (Fig. 2). We next investigated whether PaPlaB is associated with inner or outer membranes of *E. coli* by separation of these two membranes using ultracentrifugation in a sucrose density gradient. Analysis of UV absorbance (A_{280nm}) through the gradient after the centrifugation suggested an efficient separation of inner and outer membranes, which we assigned to be fraction 5 (inner membranes) and fractions 10-11 (outer membranes) (Fig. 3a). The refractometric measurement showed that the sucrose concentration in fractions 5 and 11 was 45

382 and 67 % (w/v), respectively, which is in agreement with the literature [54]. We confirmed that
383 fractions 10-11 contain the outer membrane proteins by immunodetection of outer membrane
384 protein TolC from *E. coli*, whereas fraction 5 did not contain *E. coli* TolC (Fig. 3b). Immunodetection
385 of PaPlaB revealed a weak PaPlaB signal in fraction 5 and a strong signal in fractions 10-11.
386 However, the highest esterase activity was detected for fraction 5, while the enzymatic activity of
387 the PaPlaB-enriched fraction 11 was negligibly higher than the activity of the empty vector control
388 (Fig. 3c).

389 For protein isolation, we used Triton X-100 detergent for extraction of PaPlaB from the
390 membranes, while mild, non-ionic detergent DDM was added to the buffers used for IMAC
391 purification to maintain the soluble state of PaPlaB. Elution of PaPlaB from Ni^{2+}-NTA column with
392 buffer containing an increasing concentration of imidazole resulted in highly pure PaPlaB as judged
393 from SDS-PAGE (Fig. 4). The established protocol yielded ~0.25 mg of PaPlaB per 1 l of
394 overexpression culture. Purified PaPlaB showed specific esterase (*p*-NPB substrate) and
395 phospholipase A (1,2-dilauroyl phosphatidylcholine, $PC_{12:0}$ substrate) activities of 3.41 ± 0.1 and
396 6.74 ± 0.8 *U*/mg, respectively.

397 As ethylenediaminetetraacetic acid (EDTA), an inhibitor of metal-dependent enzymes, did not
398 exert an inhibitory effect on PaPlaB (Fig. S7), we concluded that PaPlaB belongs to metal ion
399 independent type of PLAs [55]. We furthermore examined inhibition of PaPlaB activity with two
400 irreversible inhibitors, paraoxon and phenylmethylsulfonyl fluoride (PMSF). Under the conditions
401 used, the activity of the paraoxon-treated PaPlaB was abolished (Fig. S7). Paraoxon covalently
402 modifies the catalytic serine residue in the serine-hydrolase enzyme family [56]; therefore, we
403 concluded that PaPlaB contains a nucleophilic serine in its active site, which is in agreement with
404 the sequence-based prediction of a Ser-His-Asp catalytic triad (Fig. 1) and mutational studies (Fig.
405 S6). Although PMSF is also utilized to identify serine hydrolases [57], it did not inhibit the PaPlaB.

406 Paraoxon is an organophosphate inhibitor that mimics, after the reaction with an enzyme, the first
407 transition state. In contrast, PMSF is a sulfonyl inhibitor that mimics, after the reaction, the
408 transition state formed by the deacylation of the acyl-enzyme in the second step of ester-
409 hydrolysis [57]. The observed striking difference in the reactivity of paraoxon and PMSF with
410 PaPlaB may be due to differences in the stability of the two transition state mimics.

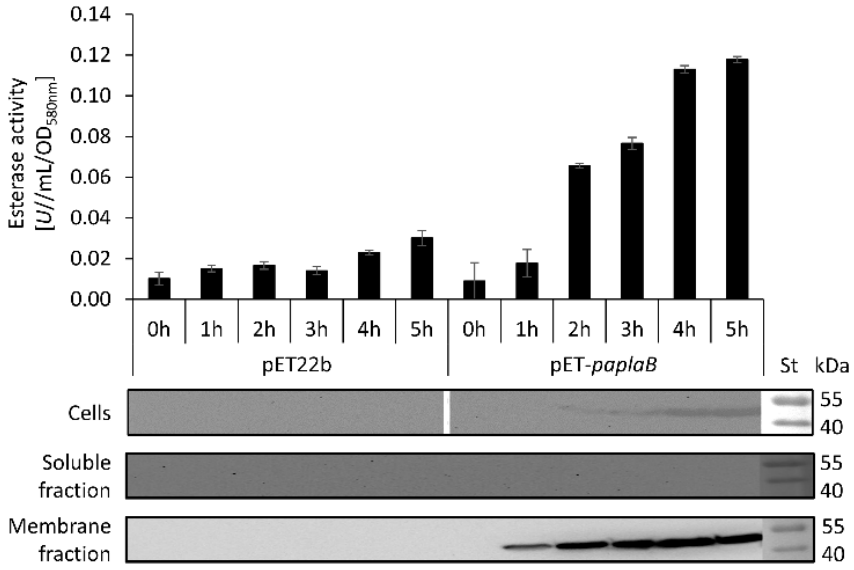

411

412 **Fig. 2: PaPlaB is heterologously expressed in *E. coli*.** Expression, localization, and activity of PaPlaB was
413 tested at 1, 2, 3, 4, and 5 h after induction. Cell lysates (10 µl, OD_{580nm} = 10) were analyzed by esterase *p*-
414 NPB assay (top) and Western blotting against the His_6-tag (below). Disrupted cells were fractionated by
415 ultracentrifugation into soluble (cytoplasmic and periplasmic proteins) and membrane protein fractions
416 that were analyzed by Western blotting. *E. coli* C43(DE3) carrying empty vector pET22b were grown under
417 the same conditions and were used as the negative control. Molecular weights of standard proteins (St) are
418 indicated on the right-hand side. The esterase activity results are means ± S.D. of three independent
419 experiments, each set in triplicate.

420

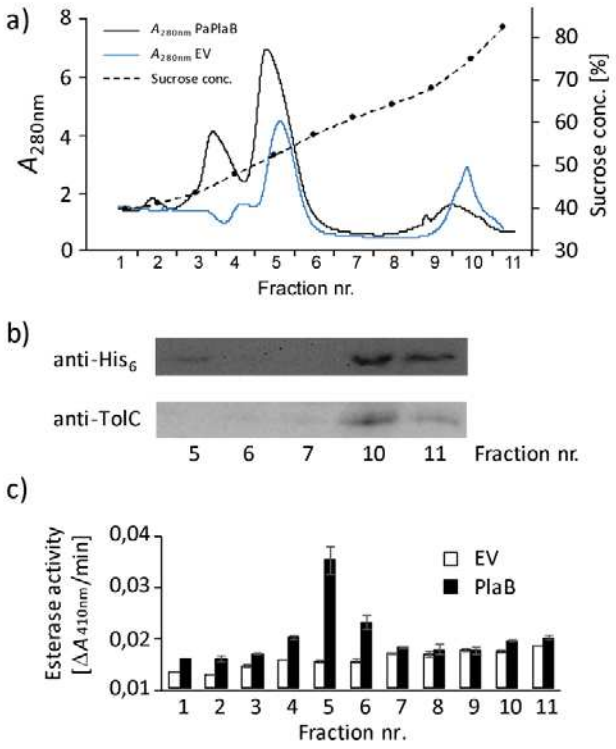

Fig. 3: Membrane localization of PaPlaB. a) Isolated membranes of *E. coli* C43(DE3) pET-*paplaB* strain cultivated in LB medium (25 ml, 5 h, 37°C) were separated by sucrose density gradient. *E. coli* C43(DE3) pET22b cultivated under the same conditions was used as the empty vector (EV) control. Fractions (1 ml) were collected and their sucrose concentration was measured refractometricaly (filled circles, dashed line). Protein absorption at 280 nm is shown in solid lines. **b)** Sucrose density gradient fractions of *E. coli* C43(DE3) pET-*paplaB* were analyzed by Western blotting using the anti-His (C-term)-HRP antibody for detection of PaPlaB and primary anti-TolC antibodies combined with the anti-rabbit immunoglobulin G antibodies for detection of TolC. **c)** Enzymatic activity was measured with *p*-NPB assay by combining 10 µl of fraction and 150 µl of the substrate. The activities are means ± S.D. of two independent experiments with three samples.

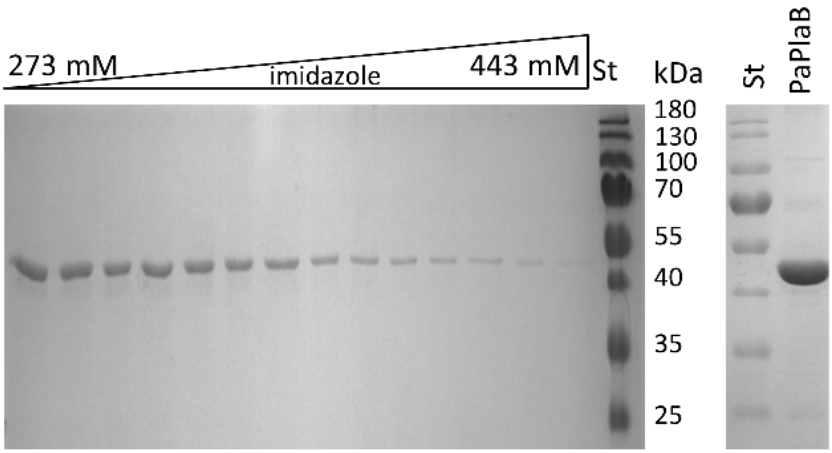

433

434 **Fig. 4: Purification of detergent-isolated PaPlaB.** The fractions eluted from the Ni-NTA column (left) and
435 pooled PaPlaB after desalting by PD-10 column (right) were analyzed by SDS-PAGE (12 % v/v). The
436 molecular weights of protein standards (St) are indicated.

437

438 ### 3.3 PaPlaB shows promiscuous PLB and lysoPLA activities

439 Using an esterase activity assay, we observed that PaPlaB retained 100 % of its activity after
440 incubation for 1 h at temperatures up to 42.5°C (Fig. S8). The thermal stability of PaPlaB was
441 confirmed by monitoring its thermal unfolding via changes in the intrinsic fluorescence. The
442 unfolding profile of PaPlaB revealed the transition temperature of ~53°C (Fig. S8). Hence, PaPlaB is
443 stable and active at temperatures relevant to bacterial infections. Therefore, a temperature of
444 37°C was used for activity assays. We next examined the PLA activity of PaPlaB using a spectrum of
445 glycerophospholipids (GPLs) naturally occurring in cell membranes. We showed that PaPlaB is a
446 rather promiscuous PLA, using GPL substrates with various head groups (ethanolamine, glycerol,
447 and choline) (Fig. 5a) and different fatty acid chain lengths (C6 – C18) (Fig. 5b). It released fatty
448 acids from all tested substrates with specific activities in the range from 2 *U*/mg to 8 *U*/mg, with
449 1,2-dimyristoyl-phosphatidylethanolamine ($PE_{14:0}$) being the best substrate. We then analyzed
450 whether PaPlaB hydrolyses GPLs containing one fatty acid linked to the *sn*-1 position called
451 lysoglycerophospholipids (lysoGPLs). Experiments using lysoGPLs with various head groups

(ethanolamine, glycerol, and choline) showed that all three lipid types were accepted as substrates by PaPlaB (Fig. 5c). Notably, the lysoPLA activity of PaPlaB is generally lower (2 – 2.5 *U*/mg) than its PLA activity toward the respective GPLs (Fig. 5c). To analyze whether PaPlaB shows specificity for hydrolysis of fatty acids bound to *sn*-1 or *sn*-2 in GPLs, artificial fluorogenic substrates (PED-A1 for PLA1, and Red/Green BODIPY® PC-A2$_{R/G}$ for PLA2) were used. These substrates contain one alkyl group bound to glycerol by ether bond, which cannot be cleaved by PLA. Both substrates were not hydrolyzed by PaPlaB (Fig. S9), most likely due to steric hindrance caused by the bulky fluorescent dyes linked to the acyl chain of substrates. We furthermore tested whether PaPlaB hydrolyzes the natural phospholipid 1-oleoyl-2-palmitoyl-PC (PC$_{18:1\text{-}16:0}$), which contains different fatty acids bound to glycerol. Spectrophotometric quantification of the total fatty acid amount after incubation of PaPlaB (4.3 µg/ml) with PC$_{18:1\text{-}16:0}$ (0.5 mM) showed PaPlaB activity of 3.7 ± 0.6 *U*/mg. To identify which fatty acids were released, PaPlaB-treated PC$_{18:1\text{-}16:0}$ samples were analyzed by GC-MS. The results of GC-MS quantification revealed 1.6 ± 0.2 µmol and 1.7 ± 0.1 µmol for palmitic and oleic acid, respectively (Table S5). This result confirmed that PaPlaB hydrolyzes both ester bonds in PC$_{18:1\text{-}16:0}$ substrate with a similar efficiency, which classifies it into the phospholipase B (PLB) family.

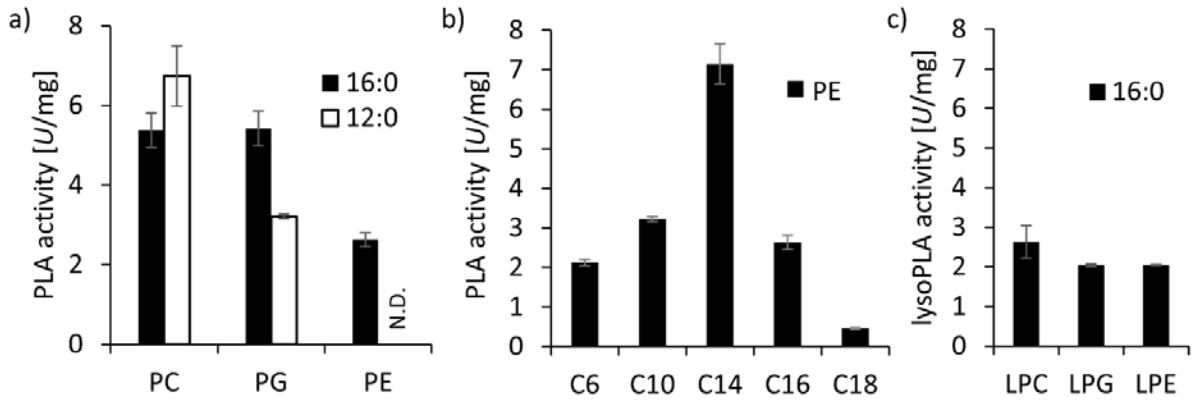

Fig. 5: Phospholipolytic activity profile of PaPlaB. **a)** PaPlaB is a PLA that hydrolases PE, PG, and PC, which contain unsaturated FAs with C16 (16:0), and C12 (12:0) chain length commonly occurring in *P. aeruginosa* membranes. N.D. = not determined. **b)** Substrate specificity of PaPlaB measured with PE containing different FA chain lengths (C6 - C18). **c)** PaPlaB shows hydrolytic activity towards various lysophospholipids (LPE, LPG, and LPC) containing unsaturated FA with C16 (16:0) chain length. PLA and lysoPLA activities were measured by NEFA-assay using 54 ng PaPlaB per reaction. Activities are mean ± S.D. of three independent experiments with three samples.

3.4 PaPlaB oligomerizes in solution

Reversible formation of dimeric and tetrameric LpPlaB was observed at protein concentrations ranging from ~0.01 to 1 mg/ml. Therefore, we assessed whether purified and DDM-stabilized PaPlaB oligomerizes in solution. Size-exclusion chromatography (SEC) analysis of PaPlaB at 0.1, 0.5, and 1.0 mg/ml revealed presence of several oligomeric PaPlaB species. Protein species of ~45 kDa, and ~360 kDa, as judged through comparison with standard globular proteins of known molecular weights, were observed for all tested PaPlaB concentrations (Fig. 6a). According to the theoretical M_w of PaPlaB of 49.5 kDa, we interpreted these as monomeric and heptameric PaPlaB, although the exact oligomerization state cannot be reliably assessed due to detergent bound to PaPlaB and likely nonglobular shape of oligomers. Notably, at low PaPlaB concentration (0.1 mg/ml), the amount of the monomeric PaPlaB is much larger than the amount of the heptameric PaPlaB, as expected. By rising the PaPlaB concentration, the equilibrium shifts towards heptamers. Additionally, PaPlaB species of intermediate molecular masses were also detected, thus indicating a stepwise oligomerization of PaPlaB. Based on the elution volumes, we assigned these oligomers to trimeric, tetrameric, and pentameric forms of PaPlaB. At high PaPlaB concentration (1 mg/ml), pentameric PaPlaB was prevalent over tetrameric and trimeric species, while at 0.5 mg/ml predominantly tetrameric, and 0.1 mg/ml predominantly trimeric PaPlaB were observed. Thus, the

equilibrium was shifted towards higher-order oligomeric species by increasing the PaPlaB concentration. The formation of homooligomers was predicted by *ab initio* docking using monomeric PaPlaB structure as an input (Fig. S10). The spatial orientation of PaPlaB monomers, dimers, and higher oligomers at the membrane suggests that PaPlaB is a peripheral membrane-bound protein (Fig. S10). This is in agreement with the negative result of the sequence-based prediction of TM helices with biological relevance (Table S6).

Determination of absolute M_w of protein:detergent complexes by SEC analysis is prone to errors. Therefore we determined the absolute M_w of DDM-stabilized PaPlaB using multi-angle light scattering coupled to SEC (MALS-SEC). The absolute M_w that was determined at a concentration of 1 mg/ml revealed a distribution starting at ~380 kDa (heptamer), which was continuously decreasing to ~50 kDa (monomer) (Fig. 6b). For the PaPlaB sample with 0.1 mg/ml very broad MALS signal in the range expected for proteins with M_w ~50 kDa was observed (Fig. S11). Similar to SEC experiments, MALS-SEC results showed that the equilibrium of PaPlaB oligomers expectedly depends on the protein concentration.

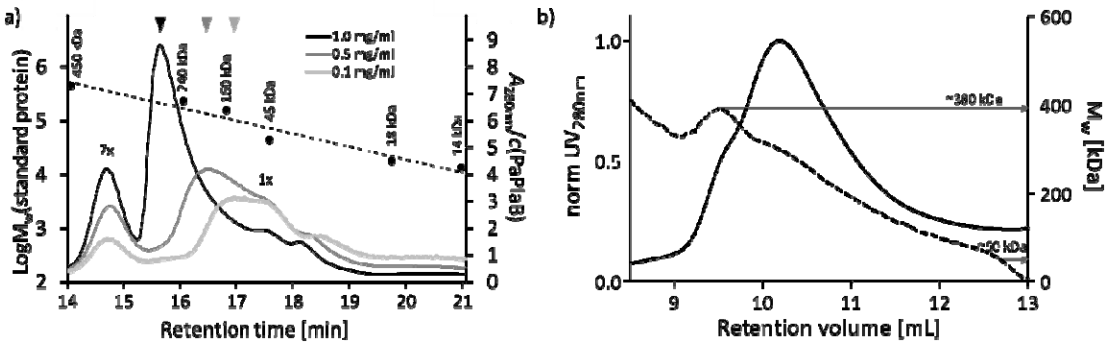

Fig. 6: Concentration-dependent oligomerization of PaPlaB. a) PaPlaB (1.0, 0.5, and 0.1 mg/ml), and standard proteins (Table S3) dissolved in a buffer containing DDM were separately analyzed using Biosep-SEC-S3000 column. Proteins were detected by measuring absorbance at 280 nm (solid curves). **b)** SEC-MALS analysis using a Superdex 200 Increase column. PaPlaB (1.0 mg/ml) stabilized by DDM was detected by

514 measuring absorbance at 280 nm (solid curve), and the overall M_w (dashed line) was determined with the
515 software ASTRA 7.

516 **3.5 PaPlaB is a major intracellular PLB of *P. aeruginosa* with hydrolytic activity towards**
517 **endogenous phospholipids**

518 To study the *in vivo* PLB function of PaPlaB in the homologous host, we constructed a *P.*
519 *aeruginosa* deletion mutant Δ*plaB,* which is missing the entire *plaB* gene (Fig. S1). The activity
520 assay showed a 60 % reduction of cell-associated PLA activity in *P. aeruginosa* Δ*plaB* compared
521 with *P. aeruginosa* wild-type (Fig. 7a). PLA activity of proteins secreted into the medium was not
522 significantly different among these two strains (Fig. 7a), indicating that PaPlaB is a cell-associated
523 and not secreted PLA of *P. aeruginosa*. PLA activity of PaPlaB demonstrated *in vitro,* and the
524 membrane localization of the enzyme provides a hint that PaPlaB might be related to hydrolysis of
525 cell membrane GPLs. To test this, we have isolated phospholipids (PLs) from the *P. aeruginosa*
526 wild-type cells by extraction with an organic solvent. These PL extracts were used at 3.3 mg/ml
527 and 0.46 mg/ml as substrates for *in vitro* PLA assay with purified PaPlaB at 450, 45, 4.5 and 0.45
528 ng/ml.
529 Results showed that PaPlaB hydrolyzes endogenous PLs with high efficiency (Fig. 7b). Hence,
530 assays with 3.3 mg/ml endogenous PLs showed comparable activities to these measured with
531 $PC_{12:0}$, which was among the best PaPlaB substrates. PaPlaB activity with endogenous PLs was
532 higher at higher substrate concentrations as expected for enzyme-catalyzed reactions. We
533 furthermore observed that specific PaPlaB activities immensely increase by diluting the PaPlaB
534 samples. Consequently, 2 and > 1100 *U*/mg activities were respectively measured with 450 and
535 0.45 ng/ml enzyme and 3.3 mg/ml endogenous PLs. We confirmed the activation of PaPlaB by
536 dilution in the assays performed with 0.46 mg/ml endogenous PLs or $PC_{12:0}$ (Fig 7b).

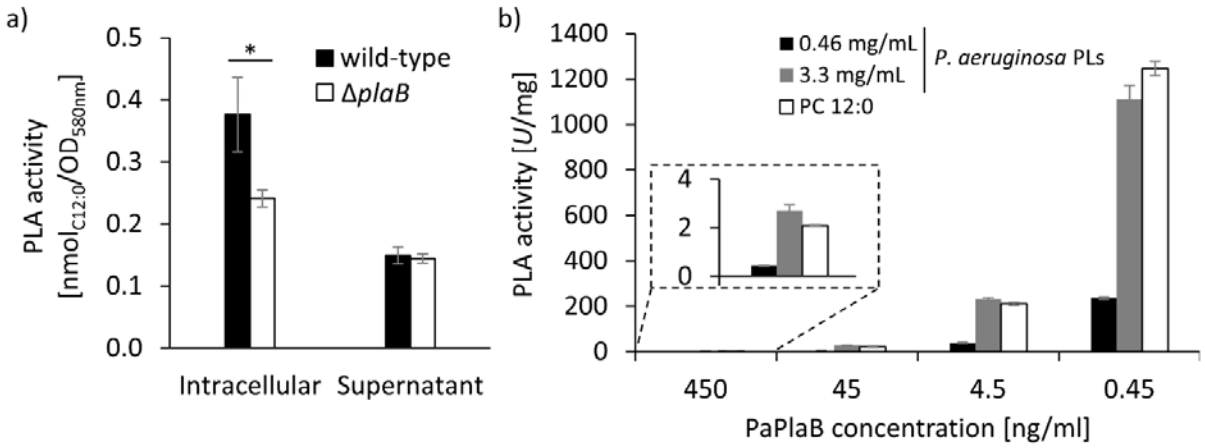

537

538 **Fig. 7: PaPlaB is an intracellular PLA of *P. aeruginosa* that releases fatty acids from endogenous**
539 **phospholipids.** a) PLA activity of the whole cells and the supernatant of *P. aeruginosa* wild-type and Δ*plaB*
540 cultivated in LB medium overnight at 37°C. Cells washed with fresh LB medium were disrupted by
541 ultrasonication before measurement. NEFA assay with $PC_{12:0}$ substrate (25 µl) was performed using cell
542 lysates (25 µl) adjusted to OD_{580nm} = 10 or undiluted cell-free supernatant (25 µl). Results are the means ±
543 S.D. of three measurements with three biological replicates. Statistical analysis was performed using the *t*-
544 test, * $p < 0.05$. b) PLA activity of purified PaPlaB was measured by NEFA assay using endogenous PLs
545 isolated from *P. aeruginosa* wild-type cells and synthetic $PC_{12:0}$, which was used as control. Free fatty acids
546 were quantified after 15 min incubation of PaPlaB with the substrate at 37°C. Activities are mean ± S.D. of
547 three measurements with three biological replicates.

548

549 ### 3.6 PaPlaB affects biofilm amount and architecture

550 To investigate whether PaPlaB affects the formation, maturation, and dispersion of biofilm, we
551 have performed long-time studies (8 – 216 h) of biofilm formation in microtiter plates (MTP) under
552 static conditions (crystal violet assay) and in the chamber with a continuous supply of the
553 nutrients under dynamic conditions (confocal laser scanning microscopic (CLSM) analysis) (Figs. 8a
554 and 8b). *P. aeruginosa* Δ*plaB* produces significantly less biofilm under static conditions than the
555 wild-type strain after 8, 24, 48, and 72 h of growth, indicating that PaPlaB plays a role in initial

556 attachment and maturation [58, 59] of *P. aeruginosa* biofilm (Fig. 8a). Under these conditions, the
557 biofilm amount in *P. aeruginosa* Δ*plaB* and wild-type cultures grown for 6 and 9 days showed no
558 significant difference, indicating that PaPlaB likely does not have a function for biofilm dispersion.
559 Based on these results, we examined the biofilm assembly of 24, 72, and 144 h-old biofilms by
560 using CLSM [60]. Large differences between the *P. aeruginosa* Δ*plaB* and WT were observed (Figs.
561 8b and S11). After 72 h, the wild-type strain forms larger aggregates opposite to small-sized
562 aggregates observed for the Δ*plaB* strain. The lower density of 72 h-old biofilms found by CLSM
563 correlates with less biofilm quantified by crystal violet assay after 72 h of growth. Interestingly,
564 although the crystal violet assay did not reveal significant differences after six days of growth, the
565 CLSM showed differences. Hence, the wild-type nearly homogeneously and densely covered the
566 surface of the flow-cell coverslip after 144 h, whereas the Δ*plaB* strain showed less dense
567 coverage indicating impaired maturation [58, 59].

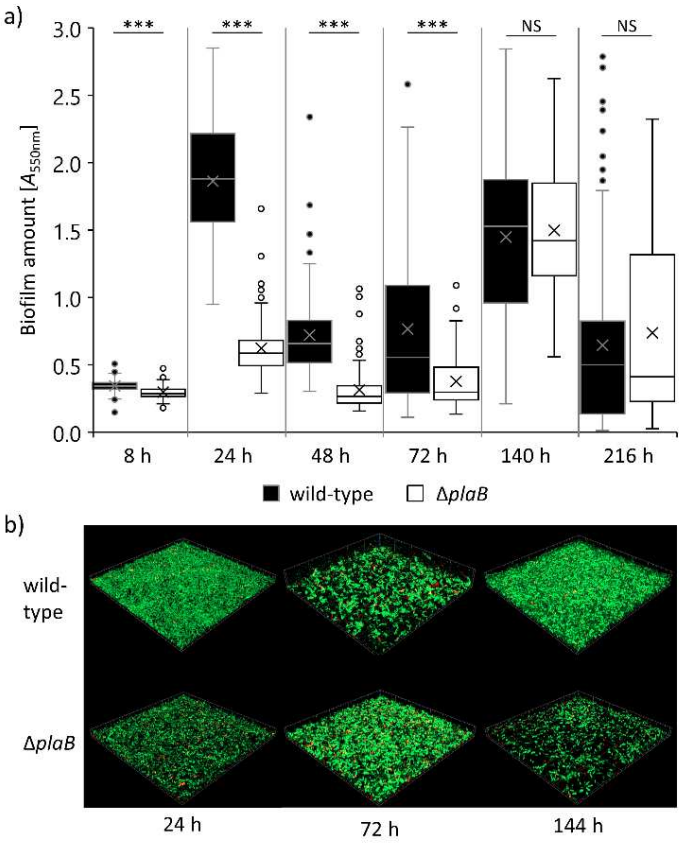

568

569 **Fig. 8: PaPlaB affects biofilm formation in *P. aeruginosa*. a)** *P. aeruginosa* wild-type and Δ*plaB* were
570 cultivated in 96-well MTP (LB medium, 37°C, without aeration). The cells not attached to the plastic surface
571 were removed, and the biofilm stained with crystal violet was quantified at 550 nm. The results are mean ±
572 S.D. of three independent experiments with five biological replicates each measured eight times. Statistical
573 analysis was performed using the *t*-test, *** $p < 0.001$. **b)** Biofilm architecture analyzed by CLSM after 24,
574 72, and 144 h growth at 37°C in a flow cell with continuous supply (50 µl/min) of LB medium. Experiments
575 were repeated two times, each with one biological replicate that was analyzed at three different points by
576 imaging a section of 100 x 100 µm. All collected images are shown in Fig. S12.
577

578 ## 4. Discussion

579 Here we identified *P. aeruginosa* PA01 gene *pa2927,* which encodes a novel PLB (PaPlaB) with a
580 function in biofilm assembly. This enzyme shows moderate global sequence homology (Fig. 1a)
581 with a known virulence-related outer membrane PLA (LpPlaB) of *L. pneumophila* [18, 19, 46, 47]
582 Sequence alignment of LpPlaB and PaPlaB revealed strongly conserved catalytic triad residues
583 (Ser, His, Asp) embraced in the N-terminal domain which is predicted to resemble α/β-hydrolase
584 fold (Fig 1b). By sequence alignment predicted and by mutational analysis confirmed (Fig. S6)
585 catalytic triad resembles in the three-dimensional model the catalytic triad reported in other Ser-
586 hydrolases with PLA activity [53]. C-terminal sequences, in contrast to N-terminal, are not similar
587 within PlaB-family and do not show similarity to other proteins (Fig. 1a). It is thought that the C-
588 terminus of the PlaB-family proteins folds into a distinct domain [18]. This was proposed for
589 LpPlaB [18] and is suggested from *de novo* structural model of PaPlaB (Fig. 1b). The functional
590 importance of the C-terminal domain was suggested, as 15 C-terminal residues were shown to
591 modulate phospholipolytic A activity of LpPlaB [46], although the reason for this is unknown.
592 Interestingly, PaPlaB is missing these 15 C-terminal residues (Fig. S2) what might be related to
593 subtle catalytic differences between LpPlaB and PaPlaB. For example, PaPlaB has comparable PLA

activities with PG and PC substrates (Fig. 5a), while LpPlaB hydrolyses PG two times faster than PC [18, 19].

We next analyzed whether PaPlaB is an intracellular or extracellular protein because the physiological function of secreted bacterial PLAs and PLBs differ substantially from the function of intracellular enzymes [7, 61]. Extracellular PLA/Bs are toxins involved in host cell membrane disruption [62] or modulation of host cell pathways through the release of bioactive compounds [7]. On the other hand, the function of intracellular PLA/Bs in bacteria is still not clearly established although we recently discovered novel cytoplasmic membrane-bound PLA1 PlaF from *P. aeruginosa* which remodeling of membrane GPLs is suggested as a virulence mechanism [9, 10]. Interestingly, the function of intracellular PLAs for the regulation of fatty acyl chain composition in GPLs through a deacylation-reacylation pathway called Lands' cycle was described in yeast [63] and other eukaryotes [64].

Using *P. aeruginosa* Δ*plaB* we observed a ~60 % reduction of a cell-associated PLA activity compared to the wild type, whereas extracellular PLA activities did not significantly differ (Fig. 7a). These results suggest that PaPlaB is the main intracellular PLA of *P. aeruginosa*. In agreement with this result is observed membrane localization of catalytically active PaPlaB recombinantly produced in *E. coli* C43(DE3) [32] (Fig. 2), although a large portion was accumulated in catalytically inactive aggregates. Furthermore, activity assays and Western blot analysis of sucrose density gradient fractionated membranes isolated from fragmented *E. coli* C43(DE3) cells overexpressing PaPlaB indicated dual membrane localization of PaPlaB (Fig. 3). Yet, only the cytoplasmic membrane fraction showed PaPlaB activity while the activity of the outer membrane fraction was comparable to the empty vector control strain. These results are only partially agreeing with the suggested outer membrane localization of LpPlaB, [46] because LpPlaB showed the highest PLA activity in outer membrane Momp protein-enriched fractions of *L. pneumophila*. However, it also

showed substantial activity (~70 % of outer membrane activity) in the fractions containing inner membranes [46]. The drawback of this fractionation method is the difficulty of absolute separation of outer from inner membranes, which was described by several research groups [46, 65, 66]. Keeping in mind that LpPlaB and PaPlaB do not have predicted TM helix or β-barrel-like structure, which were recognized in all hitherto known integral membrane proteins [67, 68], it is likely that these hydrophobic proteins are peripherally associated with one or both membranes. In line with this suggestion is our observation that monomeric PaPlaB in the presence of DDM micelles (~70 kDa large [69]) has the M_w of ~45 kDa (estimated by SEC, (Fig. 6a)) which is close to the theoretical M_w (49.5 kDa). Hence, it seems that PaPlaB has not been embedded into DDM micelle, as it would be expected for a true integral membrane protein. Additionally, the prediction of the orientation of PaPlaB at the membrane using the structural model suggests its peripheral interaction with the membrane (Fig. S10).

These findings strengthen our hypothesis that PaPlaB is rather a peripheral membrane protein. Interestingly, in PaPlaB and LpPlaB, [46] no recognizable signature for their secretion across the membrane was found; therefore, it remains unknown how these proteins are targeted across and to the membrane. Further experiments are needed to clarify cellular localization and the membrane anchoring mechanism of LpPlaB and PaPlaB.

The additional similarity of LpPlaB and PaPlaB is the phenomenon that these proteins homooligomerize at high concentrations, which is accompanied by a decrease in their enzyme activity (Fig. 7b) [47]. Using the SEC method, we observed the equilibrium of PaPlaB monomers and several oligomeric species with M_w of up to ~360 kDa, likely heptamers, at concentrations 0.1, 0.5, and 1.0 mg/ml. Keeping in mind that the shape, which presumably deviates from a sphere (Figs. 1b and S10), and bound DDM molecules make a difficult precise determination of oligomeric state by SEC, we have determined an absolute M_w of PaPlaB by MALS method. MALS analyses

642 confirmed PaPlaB monomers and the formation of various oligomers of up to ~380 kDa (Fig. 6b).
643 The observation that PaPlaB:DDM species of M_w between ~45 and ~380 kDa were simultaneously
644 present in the same sample suggests a stepwise oligomerization of PaPlaB. This is in agreement
645 with the structural prediction of PaPlaB oligomers containing from 3 to 7 PaPlaB monomers.
646 SEC and MALS results revealed that increasing the PaPlaB concentration leads to the enrichment
647 of higher oligomeric species. This is similar to LpPlaB, for which were identified only
648 homotetramers at the concentration of ≥ 0.3 mg/ml and the mixture of tetramers and dimers at
649 protein concentrations ≤ 0.05 mg/ml by analytical ultracentrifugation [47]. Furthermore, the
650 oligomerization at higher protein concentrations was accompanied by a strong decrease in
651 activities of PaPlaB and LpPlaB several hundredfolds (Fig. 7b) [47], which was suggested as a
652 mechanism of protecting the host from uncontrolled degradation of own membranes [47]. The
653 activity of *P. aeruginosa* phospholipase A ExoU [70], and human PLA_2 [71], has been suggested to
654 be regulated through homomeric protein:protein interactions. However, further studies are
655 necessary to elucidate the molecular mechanism of PaPlaB activation and particularly the role of
656 the membrane for it.
657 Although LpPlaB and PaPlaB seem not to be essential for bacterial life (Fig. S1), they both affect
658 the important virulence properties of their hosts. It was suggested that the regulation of
659 intracellular replication of *L. pneumophila* is a mechanism of LpPlaB-mediated virulence [46], while
660 the regulation of biofilm maturation was suggested as a mechanism of PaPlaB-mediated virulence
661 (Fig. 8). Despite the exact molecular mechanism by which LpPlaB and PaPlaB contribute to
662 bacterial virulence is unknown, it is most likely that phospholipid-degrading activities are essential
663 for their virulence function. We have shown that PaPlaB rapidly hydrolyses PE (Fig. 5b), which is
664 the most abundant bacterial GPL [72], at the same rate as it hydrolysed GPLs extracted from the
665 membranes of *P. aeruginosa* (Fig 7b). We could show that the biochemical function of PaPlaB is

related to the complete deacylation of GPLs to fatty acids and glycerophosphoalcohol as shown by lysoPLA assay (Fig. 5c) and GC-MS analysis of fatty acid products released from $PC_{18:1\text{-}16:0}$ (Table S5).

In conclusion, the ability of PaPlaB to rapidly degrade endogenous GPLs and above-proposed membrane localization of this novel PLB of *P. aeruginosa*, suggesting that PaPlaB might modulate the molecular GPL profile of *P. aeruginosa* membranes similarly as described for PlaF [9, 10], PLA_2 from rat [73], yeast [63] and other eukaryotes [64]. This adaptive GPL modulation might indirectly affect biofilm formation of *P. aeruginosa* what goes along with findings that *P. aeruginosa* undergoes drastic changes in membrane GPL composition upon transition from the planktonic to a biofilm lifestyle [72]. Our results contribute to a still limited understanding of the virulence mechanism of PLA/B from pathogenic bacteria that may represent a previously not explored family of antibiotic targets.

Acknowledgment

This study was funded by the Deutsche Forschungsgemeinschaft (DFG, German Research Foundation) – project number 267205415 – CRC 1208 (project A01 to LS, A02 to FK, A03 to HG and A10 to AK). HG is grateful for computational support by the "Zentrum für Informations und Medientechnologie" at the Heinrich-Heine-Universität Düsseldorf and the computing time provided by the John von Neumann Institute for Computing (NIC) to HG on the supercomputer JUWELS at Jülich Supercomputing Centre (JSC) (user IDs: HKF7; HDD18). We thank Christoph Strunk and Esther Knieps-Grünhagen (Heinrich Heine University Düsseldorf, IMET) for their help with the generation of the expression plasmid and SEC analysis, respectively, Muttalip Caliskan (Heinrich Heine University Düsseldorf, IMET) for providing GPLs extract, and Prof. Karl-Erich Jaeger (Heinrich Heine University Düsseldorf, IMET) for valuable discussions.

690 **References**

691 [1] E. Tacconelli, E. Carrara, A. Savoldi, S. Harbarth, M. Mendelson, D.L. Monnet, C. Pulcini, G. Kahlmeter, J.
692 Kluytmans, Y. Carmeli, M. Ouellette, K. Outterson, J. Patel, M. Cavaleri, E.M. Cox, C.R. Houchens, M.L.
693 Grayson, P. Hansen, N. Singh, U. Theuretzbacher, N. Magrini, W.H.O.P.P.L.W. Group, Discovery, research,
694 and development of new antibiotics: the WHO priority list of antibiotic-resistant bacteria and tuberculosis,
695 Lancet Infect Dis 18 (2018) 318-327.
696 [2] M.J. Filiatrault, K.F. Picardo, H. Ngai, L. Passador, B.H. Iglewski, Identification of *Pseudomonas*
697 *aeruginosa* genes involved in virulence and anaerobic growth, Infect Immun, 74 (2006) 4237-4245.
698 [3] B.J. Werth, J.J. Carreno, K.R. Reveles, Shifting trends in the incidence of *Pseudomonas aeruginosa*
699 septicemia in hospitalized adults in the United States from 1996-2010, Am J Infect Control, 43 (2015) 465-
700 468.
701 [4] A. Crousilles, E. Maunders, S. Bartlett, C. Fan, E.-F. Ukor, Y. Abdelhamid, Y. Baker, A. Floto, D.R. Spring,
702 M. Welch, Which microbial factors really are important in *Pseudomonas aeruginosa* infections?, Future
703 Microbiol, 10 (2015) 1825-1836.
704 [5] K.E. Jaeger, F. Kovacic, Determination of lipolytic enzyme activities, Methods Mol Biol, 1149 (2014) 111-
705 134.
706 [6] M. Flores-Diaz, L. Monturiol-Gross, C. Naylor, A. Alape-Giron, A. Flieger, Bacterial sphingomyelinases and
707 phospholipases as virulence factors, Microbiol Mol Biol Rev, 80 (2016) 597-628.
708 [7] T.S. Istivan, P.J. Coloe, Phospholipase A in Gram-negative bacteria and its role in pathogenesis,
709 Microbiol, 152 (2006) 1263-1274.
710 [8] A.M. Saliba, D.O. Nascimento, M.C.A. Silva, M.C. Assis, C.R.M. Gayer, B. Raymond, M.G.P. Coelho, E.A.
711 Marques, L. Touqui, R.M. Albano, U.G. Lopes, D.D. Paiva, P.T. Bozza, M.C. Plotkowski, Eicosanoid-mediated
712 proinflammatory activity of *Pseudomonas aeruginosa* ExoU, Cell Microbiol, 7 (2005) 1811-1822.
713 [9] F. Bleffert, J. Granzin, M. Caliskan, S.N. Schott-Verdugo, M. Siebers, B. Thiele, L. Rahme, S.
714 Felgner, P. Dörmann, H. Gohlke, R. Batra-Safferling, K.-E. Jaeger[1,11] and F. Kovacic, Structural and
715 mechanistic insights into phospholipase A-mediated membrane phospholipid degradation
716 associated with bacterial virulence, PNAS, revision submitted (2021)
717 [10] F. Bleffert, J. Granzin, H. Gohlke, R. Batra-Safferling, K.E. Jaeger, F. Kovacic, *Pseudomonas aeruginosa*
718 esterase PA2949, a bacterial homolog of the human membrane esterase ABHD6: expression, purification
719 and crystallization, Acta crystallogr F, 75 (2019) 270-277.
720 [11] S. Wilhelm, A. Gdynia, P. Tielen, F. Rosenau, K.E. Jaeger, The autotransporter esterase EstA of
721 *Pseudomonas aeruginosa* is required for rhamnolipid production, cell motility, and biofilm formation, J
722 Bacteriol, 189 (2007) 6695-6703.
723 [12] L.S. Terada, K.A. Johansen, S. Nowbar, A.I. Vasil, M.L. Vasil, *Pseudomonas aeruginosa* hemolytic
724 phospholipase C suppresses neutrophil respiratory burst activity, Infect Immun, 67 (1999) 2371-2376.
725 [13] S. Wettstadt, T.E. Wood, S. Fecht, A. Filloux, Delivery of the *Pseudomonas aeruginosa* phospholipase
726 effectors PldA and PldB in a VgrG- and H2-T6SS-dependent manner, Front Microbiol, 10 (2019) 1718.
727 [14] F. Jiang, Nicholas R. Waterfield, J. Yang, G. Yang, Q. Jin, A *Pseudomonas aeruginosa* type VI secretion
728 phospholipase D effector targets both prokaryotic and eukaryotic cells, Cell Host Microbe, 15 (2014) 600-
729 610.
730 [15] A.E. Hollsing, M. Granstrom, M.L. Vasil, B. Wretlind, B. Strandvik, Prospective study of serum
731 antibodies to *Pseudomonas aeruginosa* exoproteins in cystic fibrosis, J Clin Microbiol, 25 (1987) 1868-1874.
732 [16] L.G. Rahme, E.J. Stevens, S.F. Wolfort, J. Shao, R.G. Tompkins, F.M. Ausubel, Common virulence factors
733 for bacterial pathogenicity in plants and animals, Science, 268 (1995) 1899-1902.
734 [17] K. Seipel, A. Flieger, Legionella phospholipases implicated in infection: determination of enzymatic
735 activities, Methods Mol Biol, 954 (2013) 355-365.
736 [18] J. Bender, K. Rydzewski, M. Broich, E. Schunder, K. Heuner, A. Flieger, Phospholipase PlaB of *Legionella*
737 *pneumophila* represents a novel lipase family: protein residues essential for lipolytic activity, substrate
738 specificity, and hemolysis, J Biol Chem, 284 (2009) 27185-27194.

[19] A. Flieger, K. Rydzewski, S. Banerji, M. Broich, K. Heuner, Cloning and characterization of the gene encoding the major cell-associated phospholipase A of *Legionella pneumophila*, plaB, exhibiting hemolytic activity, Infect Immun, 72 (2004) 2648-2658.
[20] S.F. Altschul, W. Gish, W. Miller, E.W. Myers, D.J. Lipman, Basic local alignment search tool, J Mol Biol, 215 (1990) 403-410.
[21] T. Hall, Ibis Biosciences, http://www.mbio.ncsu.edu/bioedit/bioedit.html, (2007).
[22] A. Drozdetskiy, C. Cole, J. Procter, G.J. Barton, JPred4: a protein secondary structure prediction server, Nucleic Acids Res, 43 (2015) W389-394.
[23] L.A. Kelley, M.J. Sternberg, Protein structure prediction on the Web: a case study using the Phyre server, Nat Protoc, 4 (2009) 363-371.
[24] D. Mulnaes, H. Gohlke, TopScore: using deep neural networks and large diverse data sets for accurate protein model quality assessment, J Chem Theory Comput, 14 (2018) 6117-6126.
[25] D.W.A. Buchan, D.T. Jones, Improved protein contact predictions with the MetaPSICOV2 server in CASP12, Proteins, 86 Suppl 1 (2018) 78-83.
[26] M. Michel, D. Menendez Hurtado, K. Uziela, A. Elofsson, Large-scale structure prediction by improved contact predictions and model quality assessment, Bioinformatics, 33 (2017) i23-i29.
[27] M. Baek, T. Park, L. Heo, C. Park, C. Seok, GalaxyHomomer: a web server for protein homo-oligomer structure prediction from a monomer sequence or structure, Nucleic Acids Res, 45 (2017) W320-w324.
[28] M.A. Lomize, I.D. Pogozheva, H. Joo, H.I. Mosberg, A.L. Lomize, OPM database and PPM web server: resources for positioning of proteins in membranes, Nucleic Acids Res, 40 (2012) D370-376.
[29] B.W. Holloway, V. Krishnapillai, A.F. Morgan, Chromosomal genetics of *Pseudomonas*, Microbiol Rev, 43 (1979) 73-102.
[30] F. Kovacic, J. Granzin, S. Wilhelm, B. Kojic-Prodic, R. Batra-Safferling, K.E. Jaeger, Structural and functional characterisation of TesA - a novel lysophospholipase A from *Pseudomonas aeruginosa*, PLoS One, 8 (2013) e69125.
[31] D.M. Woodcock, P.J. Crowther, J. Doherty, S. Jefferson, E. DeCruz, M. Noyer-Weidner, S.S. Smith, M.Z. Michael, M.W. Graham, Quantitative evaluation of *Escherichia coli* host strains for tolerance to cytosine methylation in plasmid and phage recombinants, Nucleic Acids Res, 17 (1989) 3469-3478.
[32] B. Miroux, J.E. Walker, Over-production of proteins in *Escherichia coli*: mutant hosts that allow synthesis of some membrane proteins and globular proteins at high levels, J Mol Biol, 260 (1996) 289-298.
[33] G. Bertani, Studies on lysogenesis. I. The mode of phage liberation by lysogenic *Escherichia coli*, J Bacteriol, 62 (1951) 293-300.
[34] J. Porath, J.A.N. Carlsson, I. Olsson, G. Belfrage, Metal chelate affinity chromatography, a new approach to protein fractionation, Nature, 258 (1975) 598.
[35] U.K. Laemmli, Cleavage of structural proteins during the assembly of the head of bacteriophage T4, Nature, 227 (1970) 680-685.
[36] S.D. Dunn, Effects of the modification of transfer buffer composition and the renaturation of proteins in gels on the recognition of proteins on Western blots by monoclonal antibodies, Anal Biochem, 157 (1986) 144-153.
[37] M.R. Wilkins, E. Gasteiger, A. Bairoch, J.C. Sanchez, K.L. Williams, R.D. Appel, D.F. Hochstrasser, Protein identification and analysis tools in the ExPASy server, Methods Mol Biol, 112 (1999) 531-552.
[38] P.V. da Mata Madeira, S. Zouhir, P. Basso, D. Neves, A. Laubier, R. Salacha, S. Bleves, E. Faudry, C. Contreras-Martel, A. Dessen, Structural basis of lipid targeting and destruction by the type V secretion system of *Pseudomonas aeruginosa*, J Mol Biol, 428 (2016) 1790-1803.
[39] A. Viegas, P. Dollinger, N. Verma, J. Kubiak, T. Viennet, C.A.M. Seidel, H. Gohlke, M. Etzkorn, F. Kovacic, K.E. Jaeger, Structural and dynamic insights revealing how lipase binding domain MD1 of *Pseudomonas aeruginosa* foldase affects lipase activation, Sci Rep, 10 (2020) 3578.
[40] F. Kovacic, A. Mandrysch, C. Poojari, B. Strodel, K.E. Jaeger, Structural features determining thermal adaptation of esterases, Prot Eng Des Sel, 29 (2016) 65-76.
[41] D.J. Slotboom, R.H. Duurkens, K. Olieman, G.B. Erkens, Static light scattering to characterize membrane proteins in detergent solution, Methods (San Diego, Calif.), 46 (2008) 73-82.

[42] E. Martinez-Garcia, V. de Lorenzo, Engineering multiple genomic deletions in Gram-negative bacteria: analysis of the multi-resistant antibiotic profile of *Pseudomonas putida* KT2440, Environ Microbiol, 13 (2011) 2702-2716.
[43] T. Tolker-Nielsen, C. Sternberg, Growing and analyzing biofilms in flow chambers, Current protocols in microbiology, Chapter 1 (2011) Unit 1B.2.
[44] B. Coffey, G. Anderson, Biofilm formation in the 96-well microtiter plate, in: A. Filloux, J.-L. Ramos (Eds.) Pseudomonas Methods and Protocols, vol. 1149, Springer New York, 2014, pp. 631-641.
[45] S. Banerji, P. Aurass, A. Flieger, The manifold phospholipases A of *Legionella pneumophila* - identification, export, regulation, and their link to bacterial virulence, Int J Med Microbiol, 298 (2008) 169-181.
[46] E. Schunder, P. Adam, F. Higa, K.A. Remer, U. Lorenz, J. Bender, T. Schulz, A. Flieger, M. Steinert, K. Heuner, Phospholipase PlaB is a new virulence factor of *Legionella pneumophila*, Int J Med Microbiol, 300 (2010) 313-323.
[47] K. Kuhle, J. Krausze, U. Curth, M. Rossle, K. Heuner, C. Lang, A. Flieger, Oligomerization inhibits *Legionella pneumophila* PlaB phospholipase A activity, J Biol Chem, 289 (2014) 18657-18666.
[48] C. Lang, A. Flieger, Characterisation of *Legionella pneumophila* phospholipases and their impact on host cells, Eur J Cell Biol, 90 (2011) 903-912.
[49] A. Marchler-Bauer, M.K. Derbyshire, N.R. Gonzales, S. Lu, F. Chitsaz, L.Y. Geer, R.C. Geer, J. He, M. Gwadz, D.I. Hurwitz, C.J. Lanczycki, F. Lu, G.H. Marchler, J.S. Song, N. Thanki, Z. Wang, R.A. Yamashita, D. Zhang, C. Zheng, S.H. Bryant, CDD: NCBI's conserved domain database, Nucleic Acids Res, 43 (2015) D222-226.
[50] R.D. Finn, J. Mistry, J. Tate, P. Coggill, A. Heger, J.E. Pollington, O.L. Gavin, P. Gunasekaran, G. Ceric, K. Forslund, L. Holm, E.L. Sonnhammer, S.R. Eddy, A. Bateman, The Pfam protein families database, Nucleic Acids Res, 38 (2010) D211-222.
[51] L.A. Kelley, S. Mezulis, C.M. Yates, M.N. Wass, M.J. Sternberg, The Phyre2 web portal for protein modeling, prediction and analysis, Nat Protoc, 10 (2015) 845-858.
[52] F. Kovacic, N. Babic, U. Krauss, K.-E. Jaeger, Classification of lipolytic enzymes from bacteria, in: F. Rojo (Ed.) Aerobic utilization of hydrocarbons, oils and lipids, Springer International Publishing, Cham, 2019, pp. 1-35.
[53] D.L. Ollis, E. Cheah, M. Cygler, B. Dijkstra, F. Frolow, S.M. Franken, M. Harel, S.J. Remington, I. Silman, J. Schrag, et al., The alpha/beta hydrolase fold, Protein Eng, 5 (1992) 197-211.
[54] V. Viarre, E. Cascales, G. Ball, G.P. Michel, A. Filloux, R. Voulhoux, HxcQ liposecretin is self-piloted to the outer membrane by its N-terminal lipid anchor, J Biol Chem, 284 (2009) 33815-33823.
[55] S. Ramanadham, T. Ali, J.W. Ashley, R.N. Bone, W.D. Hancock, X. Lei, Calcium-independent phospholipases A2 and their roles in biological processes and diseases, J Lipid Res, 56 (2015) 1643-1668.
[56] I.L. Asler, M. Zehl, F. Kovacic, R. Muller, M. Abramic, G. Allmaier, B. Kojic-Prodic, Mass spectrometric evidence of covalently-bound tetrahydrolipstatin at the catalytic serine of *Streptomyces rimosus* lipase, Biochim Biophys Acta, 1770 (2007) 163-170.
[57] K.H. Nam, S.J. Kim, A. Priyadarshi, H.S. Kim, K.Y. Hwang, The crystal structure of an HSL-homolog EstE5 complex with PMSF reveals a unique configuration that inhibits the nucleophile Ser144 in catalytic triads, Biochem Biophys Res Commun, 389 (2009) 247-250.
[58] K. Sauer, A.K. Camper, G.D. Ehrlich, J.W. Costerton, D.G. Davies, *Pseudomonas aeruginosa* displays multiple phenotypes during development as a biofilm, J Bacteriol, 184 (2002) 1140.
[59] O.E. Petrova, K. Sauer, A novel signaling network essential for regulating *Pseudomonas aeruginosa* biofilm development, PLoS Pathog, 5 (2009) e1000668-e1000668.
[60] C. Reichhardt, M.R. Parsek, Confocal laser scanning microscopy for analysis of *Pseudomonas aeruginosa* biofilm architecture and matrix localization, Front Microbiol, 10 (2019) 677.
[61] A.B. Russell, M. LeRoux, K. Hathazi, D.M. Agnello, T. Ishikawa, P.A. Wiggins, S.N. Wai, J.D. Mougous, Diverse type VI secretion phospholipases are functionally plastic antibacterial effectors, Nature, 496 (2013) 508-512.
[62] D.H. Schmiel, V.L. Miller, Bacterial phospholipases and pathogenesis, Microbes Infect, 1 (1999) 1103-1112.

[63] J. Patton-Vogt, A.I.P.M. de Kroon, Phospholipid turnover and acyl chain remodeling in the yeast ER, Biochim Biophys Acta Mol Cell Biol Lipids, 1865 (2020) 158462.
[64] L. Wang, W. Shen, M. Kazachkov, G. Chen, Q. Chen, A.S. Carlsson, S. Stymne, R.J. Weselake, J. Zou, Metabolic interactions between the Lands cycle and the Kennedy pathway of glycerolipid synthesis in *Arabidopsis* developing seeds, Plant Cell, 24 (2012) 4652-4669.
[65] C.D. Vincent, J.R. Friedman, K.C. Jeong, E.C. Buford, J.L. Miller, J.P. Vogel, Identification of the core transmembrane complex of the *Legionella* Dot/Icm type IV secretion system, Mol Microbiol, 62 (2006) 1278-1291.
[66] H.M. Eriksson, P. Wessman, C. Ge, K. Edwards, A. Wieslander, Massive formation of intracellular membrane vesicles in *Escherichia coli* by a monotopic membrane-bound lipid glycosyltransferase, J Biol Chem, 284 (2009) 33904-33914.
[67] A. Craney, K. Tahlan, D. Andrews, J. Nodwell, Bacterial transmembrane proteins that lack N-terminal signal sequences, PLoS One, 6 (2011) e19421-e19421.
[68] R. Koebnik, K.P. Locher, P. Van Gelder, Structure and function of bacterial outer membrane proteins: barrels in a nutshell, Mol Microbiol, 37 (2000) 239-253.
[69] D.J. Slotboom, R.H. Duurkens, K. Olieman, G.B. Erkens, Static light scattering to characterize membrane proteins in detergent solution, Methods, 46 (2008) 73-82.
[70] A. Zhang, J.L. Veesenmeyer, A.R. Hauser, Phosphatidylinositol 4,5-bisphosphate-dependent oligomerization of the *Pseudomonas aeruginosa* cytotoxin ExoU, Infect Immun, 86 (2017) e00402-00417.
[71] J.E. Burke, E.A. Dennis, Phospholipase A2 biochemistry, Cardiovasc Drugs Ther, 23 (2009) 49-59.
[72] H. Benamara, C. Rihouey, I. Abbes, M.A. Ben Mlouka, J. Hardouin, T. Jouenne, S. Alexandre, Characterization of membrane lipidome changes in *Pseudomonas aeruginosa* during biofilm growth on glass wool, PLoS One, 9 (2014) e108478.
[73] W.E.M. Lands, Lipid Metabolism, Annu Rev Biochem, 34 (1965) 313-346.

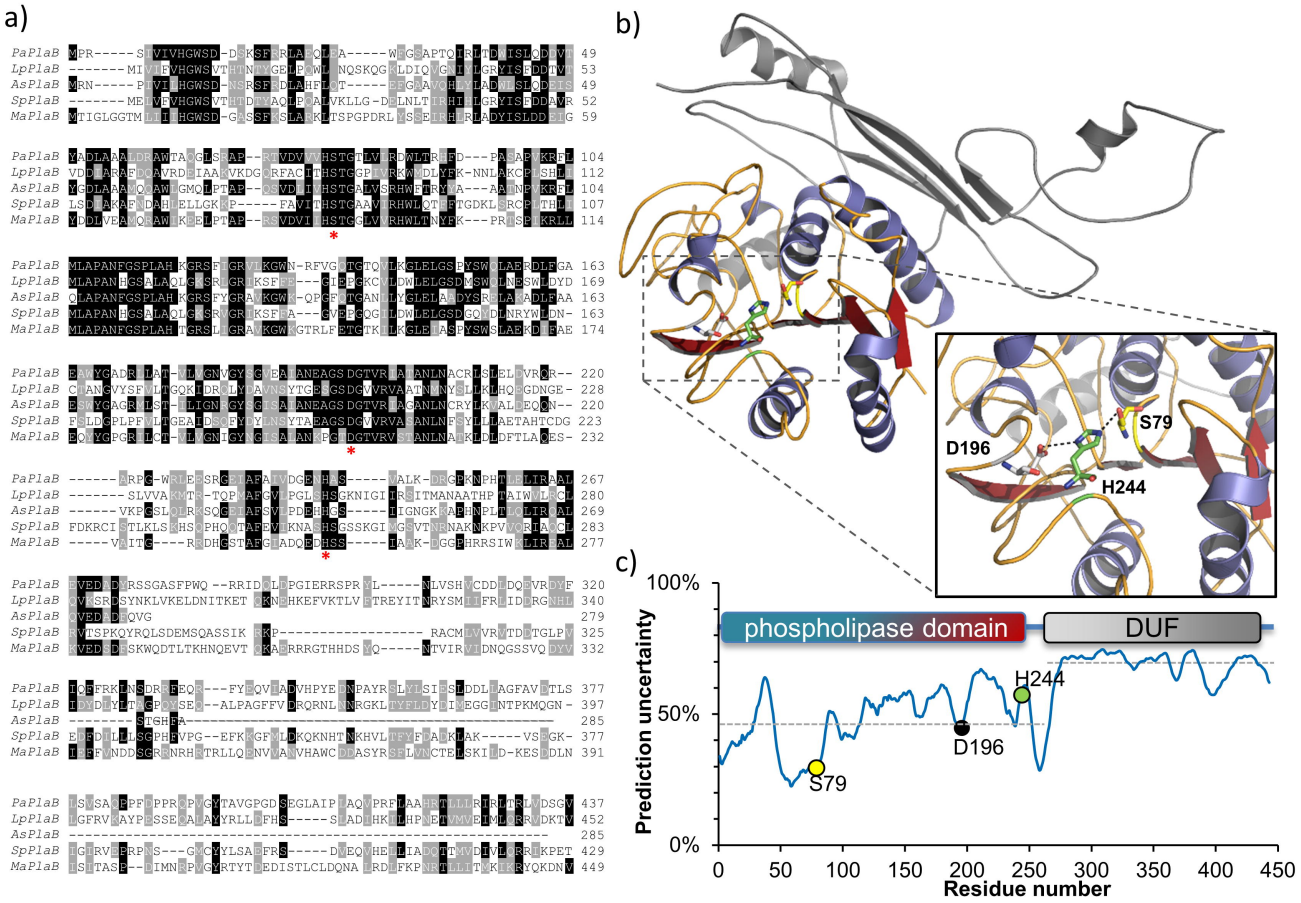
a)
b)
c)
D196
S79
H244
phospholipase domain
DUF
Prediction uncertainty
100%
50%
0%
0
50
100
150
200
250
300
350
400
450
Residue number

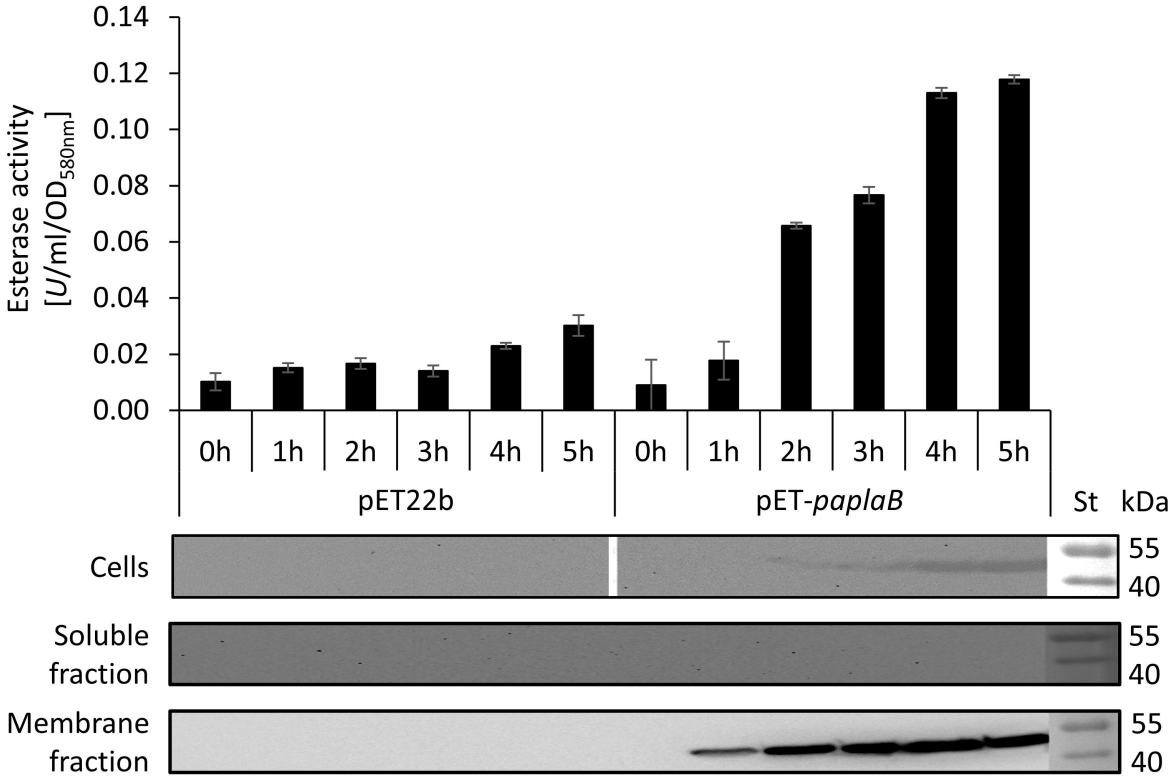
0.14
0.12
0.10
0.08
0.06
0.04
0.02
0.00
Esterase activity
[U/ml/OD580nm]
0h
1h
2h
3h
4h
5h
0h
1h
2h
3h
4h
5h
pET22b
pET-paplaB
St
kDa
Cells
Soluble fraction
Membrane fraction
55
40
55
40
55
40

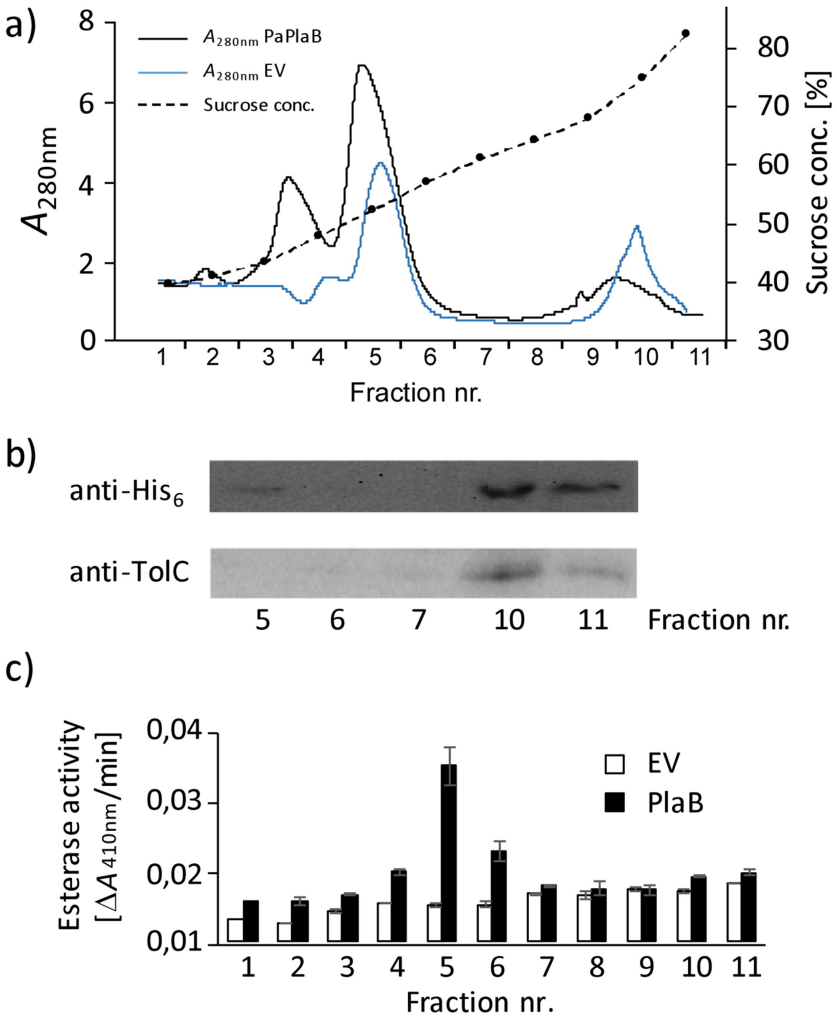
a)
A_{280nm} PaPlaB
A_{280nm} EV
Sucrose conc.
A_{280nm}
Sucrose conc. [%]
Fraction nr.
b)
anti-His$_6$
anti-TolC
5 6 7 10 11 Fraction nr.
c)
Esterase activity [ΔA_{410nm}/min]
EV
PlaB
Fraction nr.

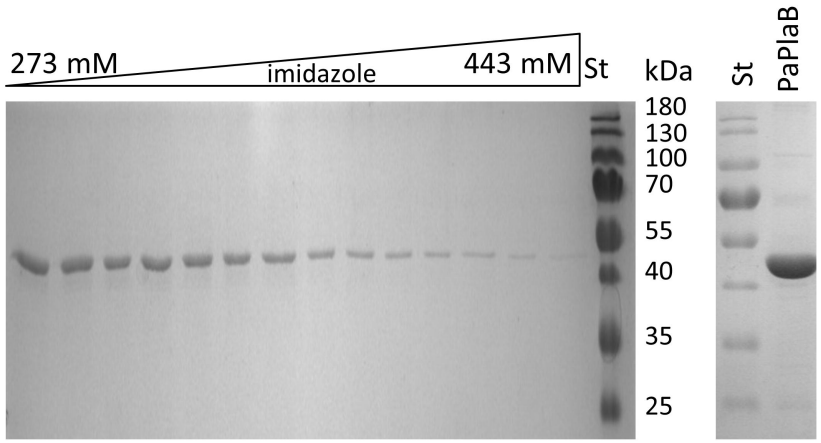
273 mM
imidazole
443 mM
St
kDa
180
130
100
70
55
40
35
25
St
PaPlaB

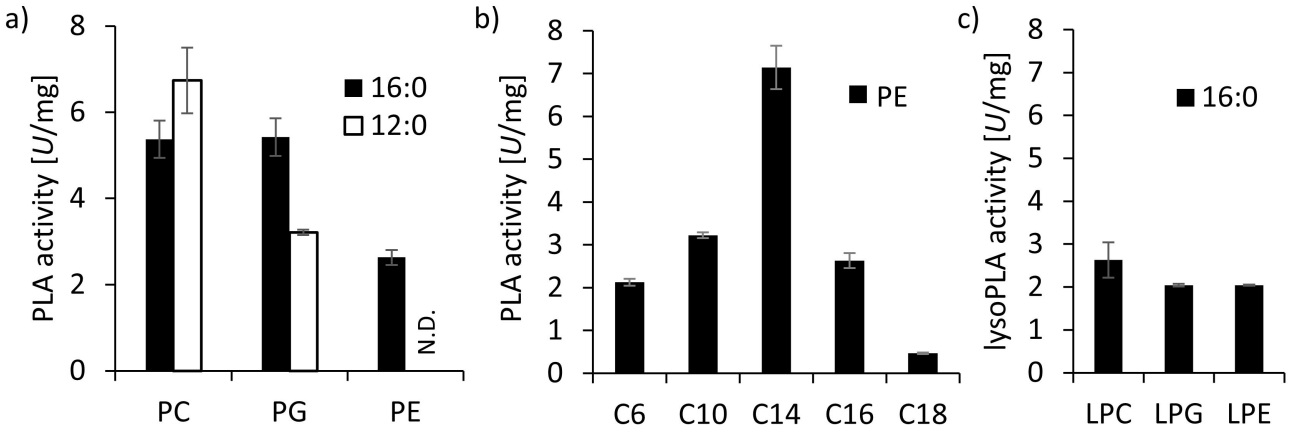
a)
PLA activity [U/mg]
16:0
12:0
N.D.
PC
PG
PE
b)
PLA activity [U/mg]
PE
C6
C10
C14
C16
C18
c)
lysoPLA activity [U/mg]
16:0
LPC
LPG
LPE

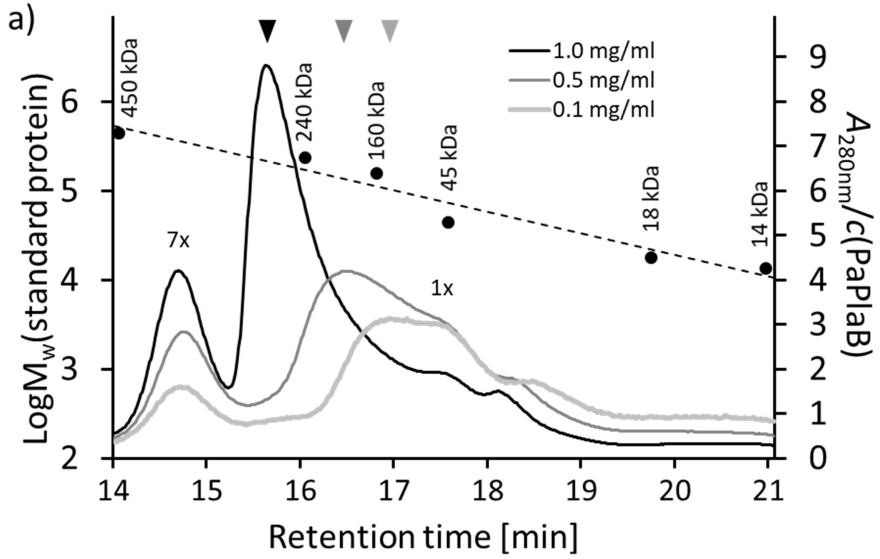
a)
1.0 mg/ml
0.5 mg/ml
0.1 mg/ml
450 kDa
240 kDa
160 kDa
45 kDa
18 kDa
14 kDa
7x
1x
LogMw(standard protein)
A280nm/c(PaPlaB)
Retention time [min]

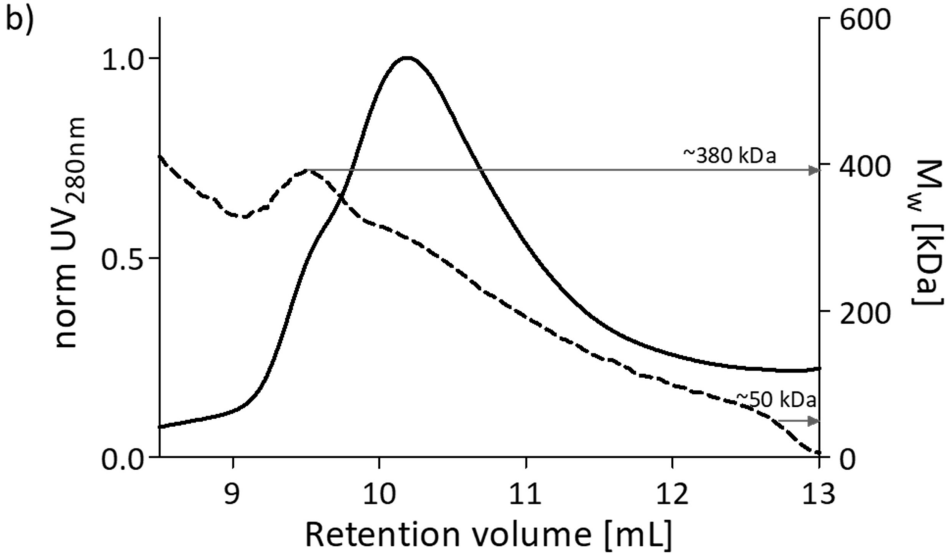
b)
~380 kDa
~50 kDa
norm UV280nm
Mw [kDa]
Retention volume [mL]

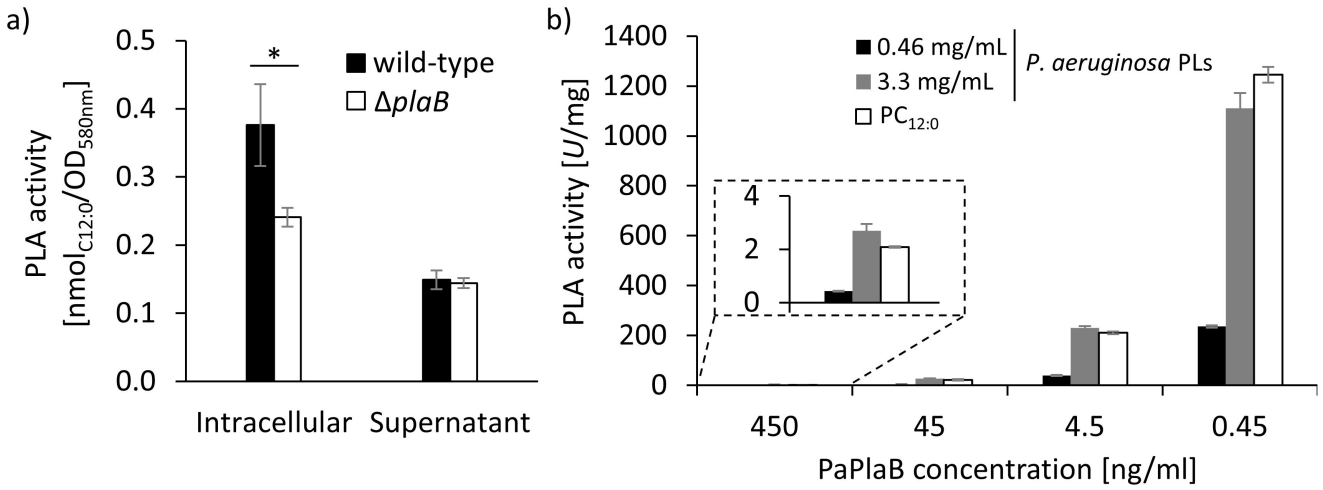
a)
PLA activity
[nmol$_{C12:0}$/OD$_{580nm}$]
0.5
0.4
0.3
0.2
0.1
0.0
*
wild-type
Δplaß
Intracellular
Supernatant
b)
PLA activity [U/mg]
1400
1200
1000
800
600
400
200
0
0.46 mg/mL
3.3 mg/mL
PC$_{12:0}$
P. aeruginosa PLs
4
2
0
450
45
4.5
0.45
PaPlaB concentration [ng/ml]

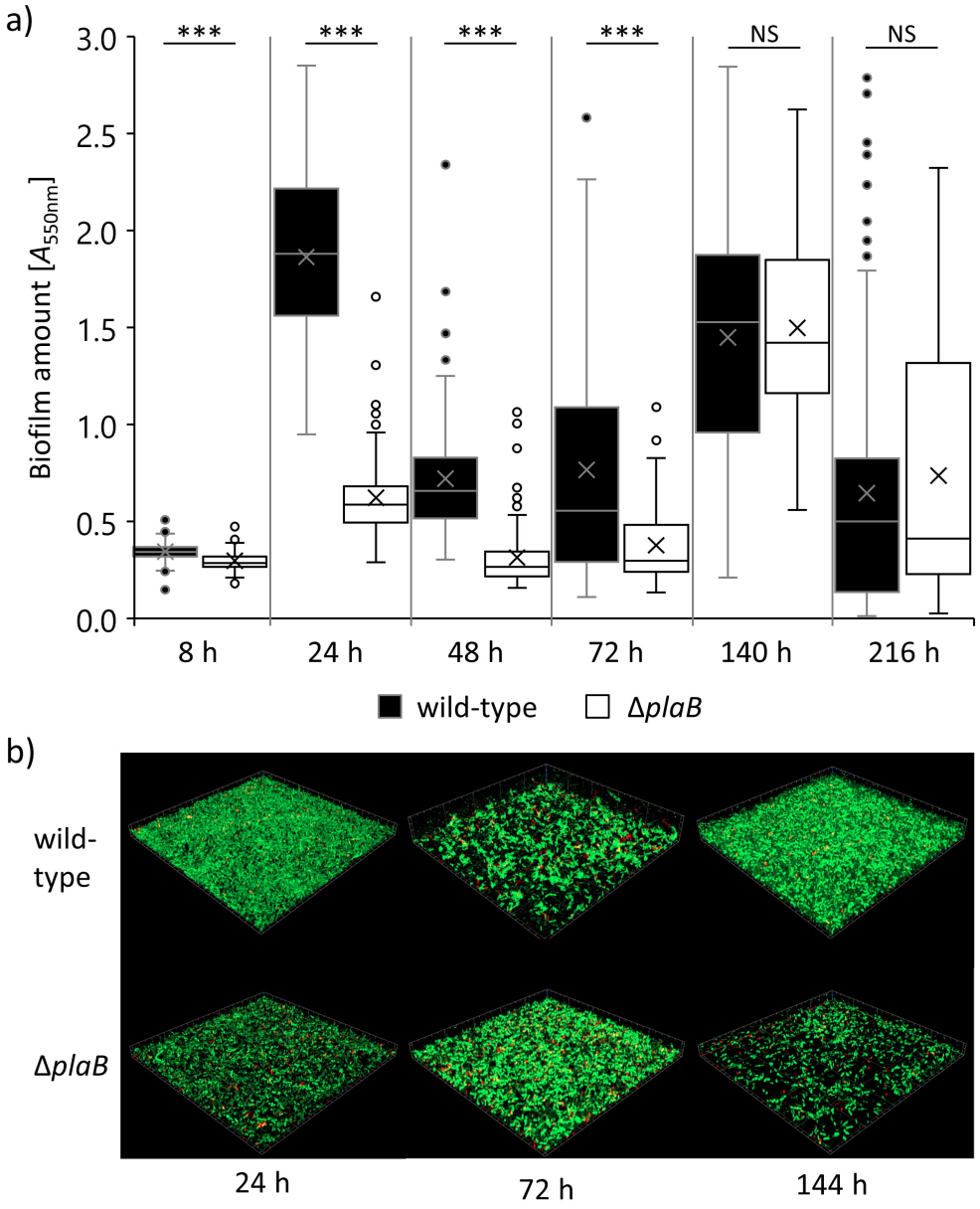
a)
***
***
***
***
NS
NS
3.0
2.5
2.0
1.5
1.0
0.5
0.0
Biofilm amount [A_{550nm}]
8 h
24 h
48 h
72 h
140 h
216 h
wild-type
ΔplaB
b)
wild-type
ΔplaB
24 h
72 h
144 h